Accurate and efficient evaluation of failure probability for partial different equations with random input data

P. Chen, A. Quarteroni

Accurate and efficient evaluation of failure probability for partial different equations with random input data

Peng Chen [1]   Alfio Quarteroni[1, 2]

Abstract: Several computational challenges arise when evaluating the failure probability of a given system in the context of risk prediction or reliability analysis. When the dimension of the uncertainties becomes high, well established direct numerical methods can not be employed because of the "curse-of-dimensionality". Many surrogate models have been proposed with the aim of reducing computational effort. However, most of them fail in computing an accurate failure probability when the limit state surface defined by the failure event in the probability space lacks smoothness. In addition, for a stochastic system modeled by partial differential equations (PDEs) with random input, only a limited number of the underlying PDEs (order of a few tens) are affordable to solve in practice due to the considerable computational effort, therefore preventing the application of many numerical methods especially for high dimensional random inputs. In this work we develop hybrid and goal-oriented adaptive reduced basis methods to tackle these challenges by accurately and efficiently computing the failure probability of a stochastic PDE. The curse-of-dimensionality is significantly alleviated by reduced basis approximation whose bases are constructed by goal-oriented adaptation. Moreover, an accurate evaluation of the failure probability for PDE system with solution of low regularity in probability space is guaranteed by the certified a posteriori error bound for the output approximation error. At the end of this paper we suitably extend our proposed method to deal with more general PDE models. Finally we perform several numerical experiments to illustrate its computational accuracy and efficiency.

Keywords: failure probability evaluation, model order reduction, reduced basis method, goal-oriented adaptation, partial differential equations, random input data

1   Introduction

In practical mathematical modeling for engineering problems, uncertainties may unavoidably arise from many sources: computational geometries, physical parameters, external loadings, etc. The evaluation of the failure probability for risk prediction or reliability analysis of a given system featuring various uncertainties or random inputs can be made by using computational methods, such as the Monte Carlo method [20], the first or second order reliability method [46, 52], the response surface method [19, 8], etc. However, efficient and accurate evaluation of failure probability is difficult to achieve, especially for a given system modeled by partial differential equations (PDEs) with high dimensional random inputs. As a matter of fact, evaluation of the output at each realization requires a complete solution of the underlying PDEs with expensive computational cost, making the direct approach of solving PDEs and evaluating outputs for a large number of realizations sampled from the high dimensional probability space prohibitive [52, 34]. Secondly, the topological and geometrical properties of the limit state surface defined by a critical failure value play a crucial role in the design of appropriate computational methods, especially when the surface lacks smoothness and/or features possible discontinuity, disconnectivity and singularity [19, 46]. At third, it is a

---

[1]Modelling and Scientific Computing, CMCS, Mathematics Institute of Computational Science and Engineering, MATHICSE, Ecole Polytechnique Fédérale de Lausanne, EPFL, Station 8, CH-1015 Lausanne, Switzerland. Peng Chen (peng.chen@epfl.ch), Alfio Quarteroni (alfio.quarteroni@epfl.ch)

[2]Modellistica e Calcolo Scientifico, MOX, Dipartimento di Matematica F. Brioschi, Politecnico di Milano, P.za Leonardo da Vinci 32, I-20133, Milano, Italy

well-known challenge of effective and efficient sampling in the evaluation of an extreme failure probability of some rare event with high consequence [8, 29]. In the present work, we are mainly dealing with the first two difficulties. The third one will be faced in a forthcoming research work by combining the computational methods developed in this work with suitable sampling techniques, such as importance sampling with efficient adaptive procedure guided by sensitivity analysis [9].

To circumvent the difficulty of directly solving the full PDE many times, efficient computational methods have been designed for constructing accurate and inexpensive surrogate models of the original PDE model. However, it has been noticed [30] that no matter how accurate the surrogate model is, the resulting failure probability evaluated via the surrogate model can be incorrect due to the non-smoothness of the limit state surface. For instance, when approximating a function by either projective or interpolative methods based on prescribed dictionary bases, the approximation error of the surrogate function can converge to zero when the number of basis functions increases. Nevertheless, the surrogate function may oscillate about the original function due to jump discontinuity because of the Gibbs phenomenon, producing therefore erroneous failure probability estimates if the discontinuity lies in the limit surface space. To deal with this problem, a hybrid approach consisting in combining the outputs computed from both the surrogate and the original models was proposed in [30]. The idea is that whenever the surrogate output is close enough to the critical value controlled by a threshold parameter, one uses the original output computed by solving the full PDE. However, the threshold parameter of the proposed direct algorithm as well as the step size and the stopping criterion of the iterative algorithm are exposed to arbitrariness, potentially leading to a biased failure probability estimate or less efficient surrogate model. When it comes to high dimensional problems, most of the surrogate models constructed by projective and interpolative approximation based on prescribed dictionary bases, run into the drawback of lower accuracy and curse-of-dimensionality. In real-world engineering problems, most of the high dimensional stochastic problems reside in a relatively low dimensional stochastic manifold named universality phenomenon [56], which provides rationality for the application of model order reduction methods to reconstruct the low dimensional manifold of the stochastic solution based on a series of snapshots, i.e. solutions at some representative samples.

In this work, we develop a hybrid and goal-oriented adaptive computational strategy based on a certified model order reduction technique - the reduced basis method [41, 50, 44, 6] - to efficiently and accurately evaluate the failure probability of a PDE with random inputs. In dealing with high dimensional random input problems, we propose and demonstrate that the reduced basis approximation space constructed by a goal-oriented greedy algorithm governed by an accurate and sharp a posteriori error bound for the output approximation error is quasi-optimal, resulting in low dimensional approximation space when the stochastic solution and output live in a low dimensional manifold. For an accurate evaluation of the failure probability when the limit state surface is non-smooth, we design a hybrid computational approach with goal-oriented adaptation. The idea is to use the surrogate model constructed by the reduced basis method to evaluate a surrogate output. If the surrogate output falls inside or outside the failure domain with certification, we do not need to solve the full PDE. Otherwise, we solve the full PDE to evaluate the original output. Since the sample of the uncertified output is very near to or in the limit state surface, we enrich the reduced basis space by the solution at this sample to build a more accurate surrogate model, especially for samples near the limit state surface. For application of the computational strategy to more general PDE models, we present several generalizations of our technique, including a primal-dual approach, a POD-greedy sampling algorithm, and an empirical interpolation algorithm for efficient decomposition of non-affine functions.

The paper is organized as follows: in section 2 we state the problem of failure probability evaluation based on a benchmark model and present several existing computational methods, followed by section 3 for the development of the hybrid and goal-oriented adaptive reduced basis methods. We extend the proposed methods to more general PDE models in section 4 and carry out a series of experiments to compare and illustrate the advantages of our methods in section 5. Concluding remarks are drawn in the last section 6.

2

2 Problem statement

We first present the generic formulation of failure probability of some quantity of interest depending on the stochastic solution of a given elliptic PDE with random inputs, then we summarize several existing computational methods.

2.1 Failure probability of PDEs

Thanks to their simplicity and generality, linear elliptic PDEs with random inputs have been widely considered as benchmark model for the development of stochastic computational methods to solve more general stochastic problems formulated as PDEs with random inputs [57, 22, 3, 33, 21, 58, 2, 36, 10, 12]. We will also start from a linear elliptic PDE with random inputs as our benchmark model and will later extend our proposed methods to more general PDE models in section 4.

Let $(\Omega, \mathcal{F}, P)$ be a complete probability space, where Ω is a set of outcomes, $\mathcal{F}$ is a σ-algebra of events and $P : \mathcal{F} \to [0, 1]$ assigns probability to the events with $P(\Omega) = 1$. Let $y = (y_1, \ldots, y_K) : \Omega \to \mathbb{R}^K$ be a random vector with each component defined as an independent and real-valued random variable with probability density function $\rho_k(y_k)$ supported on $\Gamma_k \subset \mathbb{R}, 1 \leq k \leq K$. Denote the compact forms $\rho(y) = \Pi_{k=1}^K \rho_k(y_k)$ and $\Gamma = \Pi_{k=1}^K \Gamma_k$. Let D be a convex, open and bounded physical domain in $\mathbb{R}^d$ ($d = 1, 2, 3$) with Lipschitz continuous boundary ∂D. We consider the following elliptic problem: find $u : \bar{D} \times \Gamma \to \mathbb{R}$ such that it holds almost surely for $\omega \in \Omega$

$$
\begin{aligned}
-\nabla \cdot (a(\cdot, y(\omega))\nabla u(\cdot, y(\omega))) &= f(\cdot, y(\omega)) \quad \text{in } D, \\
u(\cdot, y(\omega)) &= 0 \quad \text{on } \partial D,
\end{aligned}
\tag{2.1}
$$

where a homogeneous Dirichlet boundary condition is prescribed on the whole boundary ∂D for simplicity. $f : D \times \Gamma \to \mathbb{R}$ and $a : D \times \Gamma \to \mathbb{R}$ are random fields standing for the force term and the diffusion coefficient, respectively. The following assumptions on f and a are considered in order to guarantee the well-posedness of problem (2.1) [3, 54]:

Assumption 1 *The random force term f is square integrable with respect to the measure $\rho(y)dxdy$, i.e.*

$$
||f||_{L^2_\rho(\Gamma; L^2(D))} \equiv \int_{\Gamma \times D} f^2(x, y)\rho(y)dxdy < \infty.
\tag{2.2}
$$

Assumption 2 *The random diffusion coefficient a is assumed to be uniformly bounded from below and from above, i.e. there exist constants $0 < a_{min} < a_{max} < \infty$ such that the probability*

$$
P(\omega \in \Omega : a_{min} < a(x, y(\omega)) < a_{max} \quad \forall x \in \bar{D}) = 1.
\tag{2.3}
$$

In the context of failure probability evaluation or risk prediction, without loss of generality we are interested in computing the following probability [30]

$$
P_0 := P(\omega \in \Omega : s(u(y(\omega))) < s_0) = \int_\Gamma \mathcal{X}_{\Gamma_0}(y)\rho(y)dy,
\tag{2.4}
$$

where $s(u)$ is a functional of the stochastic solution and conventionally called limit state function or performance function in reliability problem; s_0 is a critical value defining the failure domain $\Gamma_0 := \{y \in \Gamma : s(u(y)) < s_0\}$ and the characteristic function $\mathcal{X}_{\Gamma_0}$ is defined as

$$
\mathcal{X}_{\Gamma_0}(y) = \begin{cases} 1 & \text{if } y \in \Gamma_0, \\ 0 & \text{if } y \notin \Gamma_0. \end{cases}
\tag{2.5}
$$

2.2 A quick review on existing computational methods

In order to evaluate the failure probability (2.4), we need to compute the stochastic solution of the underlying PDE (2.1) with random inputs. Various stochastic computational methods have

been developed in the last few years, such as Monte Carlo method and several variations, stochastic Galerkin method with generalized polynomial chaos, stochastic collocation method based on sparse grids, surrogate models by different model order reduction techniques, including proper spectral decomposition, reduced basis, etc. [20, 22, 59, 35, 37, 7]. Let us briefly summarize the basic ideas and properties of some different stochastic computational methods.

2.2.1   Monte Carlo method

Monte Carlo method is used to solve the stochastic system as well as evaluate the failure probability [20]. The idea is to generate a series of samples $y^m \in \Gamma$, $m = 1, 2, \ldots, M$ according to the probability density function $\rho(y)$, solve the underlying PDE problem at each sample to get the stochastic solution $u(y^m)$, compute the output of interest $s(u(y^m))$ and evaluate the failure probability (Monte Carlo failure probability, denote as P_0^m) by taking average as

$$P_0^m = \frac{1}{M} \sum_{m=1}^{M} \mathcal{X}_{\Gamma_0}(y^m). \tag{2.6}$$

The method is extremely straightforward as it requires no additional effort for modification of the deterministic solver of the PDE. However, in practical application it is too expensive because one PDE has to be fully solved for each of a large number of samples, leading in general to prohibitive computational cost. Several accelerated variations of Monte Carlo method have been developed and used in failure probability evaluation, such as quasi Monte Carlo, Latin hypercube sampling, multi-level techniques, etc. [47]

2.2.2   Stochastic Galerkin method

Stochastic Galerkin method moves from spectral expansion of both the random inputs and stochastic solution on certain type of polynomial basis, e.g. Hermite polynomials for independent Gaussian random variables, then apply the Galerkin projection, for instance in finite element space, to approximate the solution in physical space [22, 54, 3, 55]. Explicitly, we seek the stochastic solution u in the tensor product space $X_h^d \otimes Y_K^p$ such that

$$\int_{\Gamma \times D} a(x,y) \nabla u(x,y) \cdot \nabla v(x,y) \rho(y) dx dy = \int_{\Gamma \times D} f(x,y) v(x,y) \rho(y) dx dy \; \forall v \in X_h^d \otimes Y_K^p, \tag{2.7}$$

where the subspace $X_h^d \subset H_0^1(D)$ is a finite element space with mesh size h (see [45, 42]), $Y_K^p \subset L_\rho^2(\Gamma)$ is usually taken as multidimensional orthogonal polynomial space of order up to p with different settings [5] and the tensor product space $X_h^d \otimes Y_K^p$ is defined as

$$X_h^d \otimes Y_K^p := \left\{ \psi = \psi(x,y) \in H_0^1(D) \otimes L_\rho^2(\Gamma) : \psi \in \text{ span } \{\phi(x)\varphi(y) : \phi \in X_h^d, \varphi \in Y_K^p\} \right\}. \tag{2.8}$$

This method enjoys fast convergence provided the solution satisfies certain regularity [15]. It has also been extended for practical applications using generalized polynomial chaos [59] for uncertainties featuring more general distributions inspired by the mathematical coherence of different types of orthogonal polynomials and stochastic processes. However, a very large algebraic system is typically derived from the weak formulation (2.7) by stochastic Galerkin approach, which results in great computational challenge of designing efficient solvers [17].

2.2.3   Stochastic collocation method

Stochastic collocation method was developed from the non-intrusive deterministic collocation method [45]. In principle, it employs multivariate polynomial interpolations for the integral in the variational formulation of the stochastic system with respect to probability space rather than the Galerkin approximation in the spectral polynomial space [58, 2].More precisely, taking a sequence

of collocation nodes $y^1, y^2, \ldots$, we solve a deterministic problem for each node $y^n, n = 1, 2, \ldots$

$$\int_D a(x, y^n) \nabla u(x, y^n) \cdot \nabla v(x) dx = \int_D f(x, y^n) v(x) dx \quad \forall v \in X_h^d, \tag{2.9}$$

then apply multidimensional interpolation formula to approximate the stochastic solution at any other node $y \in \Gamma$. In order to alleviate the curse-of-dimensionality in high dimensional problems, isotropic or anisotropic sparse grids with suitable cubature rules [35, 34] were applied for stochastic collocation method to reduce the total computational effort. The sparse grid interpolation formula is written as

$$\mathcal{S}_q u(y) = \sum_{q-K+1 \leq |i| \leq q} (-1)^{q-|i|} \begin{pmatrix} K-1 \\ q-|i| \end{pmatrix} \left(\mathcal{U}^{i_1} \otimes \cdots \otimes \mathcal{U}^{i_K} \right) u(y), \tag{2.10}$$

where $\mathcal{U}^{i_k}$ is one dimensional interpolation formula with collocation nodes defined via index $i_k, 1 \leq k \leq K$ that are bounded by the interpolation order q [35, 34]. This method is preferred to the stochastic Galerkin one for practical applications because it combines the advantages of both direct computation as Monte Carlo method and fast convergence as stochastic Galerkin method.

2.2.4 Model order reduction method

Model order reduction methods for stochastic problems aim at building a reduced basis approximation space for the stochastic solution in such a way that the error between the true solution u and the approximate solution u_M is minimized with respect to a given norm $|| \cdot ||$ [37], i.e.

$$||u - u_M|| = \min_{\substack{\{w_m\}_{m=1}^M \in (H_0^1(D))^M \\ \{\lambda_m\}_{m=1}^M \in (L_\rho^2(\Gamma))^M}} \left\| u - \sum_{m=1}^M w_m \lambda_m \right\|, \tag{2.11}$$

where the approximate solution u_M is obtained by solving a Galerkin projection problem in the reduced basis approximation space. However, the optimal approximation (2.11) is usually not achievable in practice due to the fact that the stochastic and deterministic spaces are both infinite dimensional spaces. How to cheaply and optimally build the reduced basis space is critical for the computational effectivity and efficiency of model order reduction methods. This is where different model order reduction techniques, such as generalized spectral decomposition [36, 38], reduced basis construction by greedy algorithm, proper orthogonal decomposition, Krylov subspace, etc. [50, 32, 51, 37, 6, 12], diverge one another.

3 Reduced basis methods

To develop hybrid and goal-oriented adaptive reduced basis methods, we first introduce the reduced basis method based on the benchmark model (2.1), then we propose a hybrid approach for evaluation of the failure probability guided by a posteriori error bound. Finally, we present a goal-oriented adaptive reduced basis method for efficient evaluation of the failure probability.

3.1 Reduced basis method

Nowadays, reduced basis method represents one of the most efficient model order reduction techniques [50, 41, 25, 24] in many engineering applications [43, 14, 44, 28, 49]. For ease of its presentation, we make the following affine assumption for the random fields a, f based on the elliptic PDE model (2.1), then we remove it later in section 4.

Assumption 3 *The random fields a and f can be decomposed into finite affine terms as*

$$a(x, y) = \sum_{q=1}^{Q_a} \Theta_q^a(y) a_q(x) \ and \ f = \sum_{q=1}^{Q_f} \Theta_q^f(y) f_q(x), \tag{3.1}$$

where Q_a, Q_f are the number of affine terms, Θ_q^a, Θ_q^f are random functions in the probability space and a_q, f_q are deterministic functions in the physical space.

Remark 3.1 *The assumption of finite affine decomposition of a random field is most often made in practical stochastic modeling and statistical analysis [3, 33, 21, 2, 36]. In fact, any random field with finite second moment can be decomposed into a finite number of affine terms by truncated Karhunen-Loève expansion [53].*

Under assumption 3, the semi-weak (only in deterministic space) formulation of the elliptic problem (2.1) can be written as: for any $y \in \Gamma$, find $u(y) \in H_0^1(D)$ such that

$$A(u, v; y) = F(v; y) \quad \forall v \in H_0^1(D), \tag{3.2}$$

where the bilinear form $A(u, v; y)$ and the linear form $F(v; y)$ are split as

$$A(u, v; y) = \sum_{q=1}^{Q_a} \Theta_q^a(y) A_q(u, v) \text{ and } F(v; y) = \sum_{q=1}^{Q_f} \Theta_q^f(y) F_q(v), \tag{3.3}$$

being $A_q(u, v) = (a_q \nabla u, \nabla v) = \int_D a_q \nabla u \cdot \nabla v dx, 1 \leq q \leq Q_a$ and $F_q(v) = (f_q, v) = \int_D f_q v dx, 1 \leq q \leq Q_f$. The general paradigm of reduced basis method is formulated as: given any subspace $X \subset H_0^1(D)$ of dimension $\mathcal{N}$ (for instance, a high fidelity finite element space) for the approximation of the solution of problem (3.2) in the physical space, we hierarchically build an N dimensional reduced basis space $X_N = \text{span}\{u(y^n), 1 \leq n \leq N\}$ for $N = 1, \ldots, N_{max}$ until satisfying certain tolerance requirement at $N_{max} \ll \mathcal{N}$, based on the samples $S_N = \{y^1, \ldots, y^N\}$ suitably chosen from a training set $\Xi_{train} \subset \Gamma$. Given any new sample $y \in \Gamma$, we seek the solution $u_N(y)$ in the reduced basis space X_N by solving

$$A(u_N, v; y) = F(v; y) \quad \forall v \in X_N, \tag{3.4}$$

then evaluate $s_N(y) = s(u_N(y))$ in order to compute the failure probability in (2.4). To select the most representative sample set S_N, hierarchically build the reduced basis space X_N, and efficiently evaluate the output s_N with certification, three specific ingredients of the reduced basis method play a key role, being greedy algorithm, a posteriori error bound construction and an offline-online computational decomposition, which are addressed respectively as follows.

3.1.1 Greedy algorithm

The greedy algorithm essentially deals with the following $L^\infty(\Gamma; X)$ optimization problem [50]

$$y^N = \arg\sup_{y \in \Gamma} ||u(y) - u_{N-1}(y)||_X, \quad N = 2, \ldots, N_{max}, \tag{3.5}$$

from which we can find the least matching point (the point where the approximation error is the largest) $y^N \in \Gamma$ by reduced basis approximation in $|| \cdot ||_X$ norm. In order to solve problem (3.5) efficiently, we replace the probability domain Γ by a finite training sample set $\Xi_{train} \subset \Gamma$ and the approximation error $||u(y) - u_{N-1}(y)||_X$ by the help of an a posteriori error bound $\triangle_{N-1}$ that should be as cheap and sharp as possible, i.e.

$$c_{N-1} \triangle_{N-1}(y) \leq ||u(y) - u_{N-1}(y)||_X \leq \triangle_{N-1}(y) \tag{3.6}$$

6

where $c_{N-1} < 1$ measures the sharpness. For the sake of efficient computation of the approximation u_N and a posteriori error bound $\triangle_N$, we orthonormalize the reduced basis functions in X_N by Gram-Schmidt process (when N becomes large and $\triangle_N$ becomes critically small, two iterations of GS process can be used to guarantee the orthonormality of the bases [23]) to get $\{\zeta_1, \ldots, \zeta_N\}$ such that $(\zeta_m, \zeta_n)_X = \delta_{mn}$, $1 \leq m, n \leq N$ and then build $X_N = \text{span}\{\zeta_1, \ldots, \zeta_N\}$.

Another algorithm that might be used for the sampling procedure is proper orthogonal decomposition, POD for short [50], which is rather expensive as it deals with $L^2(\Gamma; X)$ optimization and thus more suitable for low dimensional problems. We remark that for both the greedy and the POD algorithms, an original training set Ξ_{train} is needed. Two criteria ought be followed for its choice: 1, it should be cheap without too many ineffectual samples in order to avoid too much computation with little gain; 2, it should be sufficient to capture the most representative snapshots so as to build an accurate reduced basis space. Adaptive approaches for building the training set have also been well explored by adaptively increasing the number of samples in the probability domain Γ, see [60] for details.

3.1.2 Construction of a posteriori error bounds

Residual based a posteriori error bounds for reduced basis approximation can be obtained as follows [50, 41]: for every $y \in \Gamma$, let $R(v; y) \in X'$ be the residual in the dual space of X, defined as

$$R(v; y) := F(v; y) - A(u_N(y), v; y) \quad \forall v \in X. \tag{3.7}$$

By Riesz representation theorem [18], we have a unique function $\hat{e}(y) \in X$ such that

$$(\hat{e}(y), v)_X = R(v; y) \quad \forall v \in X, \tag{3.8}$$

and $||\hat{e}(y)||_X = ||R(\cdot; y)||_{X'}$, where the X-norm is defined as $||v||_X = A(v, v; \bar{y})$ at some reference value $\bar{y} \in \Gamma$ (we choose $\bar{y}$ as the center of Γ by convention). Defining the error $e(y) := u(y) - u_N(y)$, we have by (3.2), (3.4) and (3.7) the following equation

$$A(e(y), v; y) = R(v; y) \quad \forall v \in X. \tag{3.9}$$

By setting $v = e(y)$ and using Cauchy-Schwarz inequality, we have

$$\alpha(y)||e(y)||_X^2 \leq A(e(y), e(y); y) = R(e(y); y) \leq ||R(\cdot; y)||_{X'}||e(y)||_X = ||\hat{e}(y)||_X||e(y)||_X, \tag{3.10}$$

where $\alpha(y)$ is the coercivity constant of the bilinear form $A(e(y), e(y); y)$ at y, so that we can define the a posteriori error bound $\triangle_N^u(y)$ for the approximation error $||u(y) - u_N(y)||_X$ as

$$\triangle_N^u(y) := ||\hat{e}(y)||_X/\alpha(y), \tag{3.11}$$

yielding $||u(y) - u_N(y)||_X \leq \triangle_N^u(y)$ by (3.10). We remark that we don't consider the spatial discretization error (finite element approximation error). For the output in the compliant case, i.e. $s(y) \equiv s(u(y); y) = F(u(y); y)$, we have the following error bound

$$|s(y) - s_N(y)| = |F(u(y); y) - F(u_N(y); y)| = A(e(y), e(y); y) \leq ||\hat{e}(y)||_X^2/\alpha(y) =: \triangle_N^s(y). \tag{3.12}$$

As for more general output where $s(y) \neq F(u(y); y)$, an adjoint problem of (3.2) can be employed to achieve faster convergence of the approximation error $|s - s_N|$, which will be extended in section 4. The computation of a posteriori error bound $\triangle_N^s(y)$ for the approximation error of the output $|s(y) - s_N(y)|$ turns to the evaluation of the coercivity constant $\alpha(y)$ and the value $||\hat{e}(y)||_X$ for any given $y \in \Gamma$. For the former, we can employ the successive constraint linear optimization method (SCM) [27] to compute a random lower bound $\alpha_{LB}(y) \leq \alpha(y)$ or use a uniform lower bound $\alpha_{LB} \leq \alpha(y)$ (provided that the coercivity constants at different samples $y \in \Gamma$ are close to each other) in order to alleviate the computational effort. For the latter, we use an offline-online computational decomposition, see next subsection.

3.1.3 Offline-online computational decomposition

The reduced basis solution $u_N(y)$ can be expanded on the reduced basis functions as

$$u_N(y) = \sum_{m=1}^{N} u_{Nm}(y)\zeta_m. \tag{3.13}$$

By Galerkin projection, the problem (3.4) becomes: find $u_{Nm}(y), 1 \leq m \leq N$ such that

$$\sum_{m=1}^{N}\sum_{q=1}^{Q_a} \Theta_q^a(y)A_q(\zeta_m, \zeta_n)u_{Nm}(y) = \sum_{q=1}^{Q_f} \Theta_q^f(y)F_q(\zeta_n), \quad 1 \leq n \leq N, \tag{3.14}$$

where the matrix $A_q(\zeta_m, \zeta_n), 1 \leq q \leq Q_a, 1 \leq m, n \leq N_{max}$ and the vector $F_q(\zeta_n), 1 \leq q \leq Q_f, 1 \leq n \leq N_{max}$ can be pre-computed and stored in the offline stage. In the online stage, we only need to assemble and solve the resulting $N \times N$ stiffness system of (3.14) with much less computational effort compared to solving the original $\mathcal{N} \times \mathcal{N}$ stiffness system. The approximate compliant output $s_N(y)$ is thus evaluated by NQ_f operations (scalar multiply and sum) as

$$s_N(y) = F(u_N(y); y) = \sum_{n=1}^{N}\left(\sum_{q=1}^{Q_f} \Theta_q^f(y)F_q(\zeta_n)\right) u_{Nn}(y). \tag{3.15}$$

To evaluate $||\hat{e}(y)||_X^2$ for the computation of a posteriori error bound $\triangle_N^s(y)$ in (3.12), we first expand the residual (3.7) as

$$R(v; y) = F(v; y) - A(u_N, v; y) = \sum_{q=1}^{Q_f} \Theta_q^f(y)F_q(v) - \sum_{n=1}^{N}\left(\sum_{q=1}^{Q_a} \Theta_q^a(y)A_q(\zeta_n, v)\right) u_{Nn}(y). \tag{3.16}$$

For $\forall v \in X_N$, set $(\mathcal{C}_q, v)_X = F_q(v), 1 \leq q \leq Q_f$ and $(\mathcal{L}_q^n, v)_X = -A_q(\zeta_n, v), 1 \leq n \leq N, 0 \leq q \leq Q_a$, where $\mathcal{C}_q$ and $\mathcal{L}_q^n$ are regarded as the representatives in X whose existence is guaranteed by the Riesz representation theorem. By recalling (3.7) and (3.8) we obtain

$$\begin{aligned}||\hat{e}(y)||_X^2 &= \sum_{q}^{Q_f}\sum_{q'}^{Q_f} \Theta_q^f(y)\Theta_{q'}^f(y)(\mathcal{C}_q, \mathcal{C}_{q'})_X + 2\sum_{n=1}^{N}\sum_{q=1}^{Q_f}\sum_{q'=1}^{Q_a} \Theta_q^f(y)\Theta_{q'}^a(y)(\mathcal{C}_q, \mathcal{L}_{q'}^n)_X u_{Nn}(y) \\ &+ \sum_{n=1}^{N}\sum_{n'=1}^{N}\sum_{q=1}^{Q_a}\sum_{q'=1}^{Q_a} \Theta_q^a(y)\Theta_{q'}^a(y)u_{Nn}(y)(\mathcal{L}_q^n, \mathcal{L}_{q'}^{n'})_X u_{Nn'}(y).\end{aligned} \tag{3.17}$$

Therefore, we can pre-compute and store $(\mathcal{C}_q, \mathcal{C}_{q'})_X, 1 \leq q, q' \leq Q_f, (\mathcal{C}_q, \mathcal{L}_{q'}^n)_X, 1 \leq n \leq N, 1 \leq q \leq Q_f, 1 \leq q' \leq Q_a, (\mathcal{L}_q^n, \mathcal{L}_{q'}^{n'})_X, 1 \leq n, n' \leq N_{max}, 1 \leq q, q' \leq Q_a$ in the offline stage, and evaluate $||\hat{e}(y)||_X$ in the online stage by assembling (3.17) with $Q_f^2 + NQ_fQ_a + N^2Q_a^2$ operations.

For the evaluation of the failure probability defined in (2.4), we first compute the surrogate output s_N by reduced basis method and evaluate the surrogate failure probability by

$$P_0^s = \frac{1}{M}\sum_{m=1}^{M} \mathcal{X}_{\Gamma_0^s}(y^m), \tag{3.18}$$

where the surrogate approximate failure domain is defined as $\Gamma_0^s := \{y \in \Gamma : s_N(y) < s_0\}$.

With greedy algorithm to choose the most representative samples, a posteriori error bound to speed up greedy algorithm as well as certify the approximation accuracy, and an offline-online decomposition to profit from computational efficiency, a complete reduced basis method for computing failure probability is presented in the following Algorithm 1 (where we recall that ρ denotes

the probability density, ε_{tol} is the tolerance to stop the construction of the reduced basis space, the set Ξ_{new} is sampled independently according to the ρ in which the failure probability is evaluated):

Algorithm 1 Algorithm for reduced basis method

1: **procedure** OFFLINE CONSTRUCTION:
2:     **Initialization:** mesh, parameters, finite element functions $\phi_i, 1 \leq i \leq \mathcal{N}$, etc;
3:     pre-compute and store $A_q = A_q(\phi_., \phi_.), 1 \leq 1 \leq Q_a$ and $F_q(\phi_.), 1 \leq q \leq Q_f$;

4:     sample Ξ_{train} according to ρ, pre-compute and store $\alpha_{LB}(y), y \in \Xi_{train}$ by SCM [27];
5:     choose $y^1 \in \Xi_{train}$, solve $u(y^1)$ by (3.2), compute $\zeta_1 = u(y^1)/\|u(y^1)\|_X$,
6:     construct the first sample set $S_1 = \{y^1\}$ and reduced basis space $X_1 = \{\zeta_1\}$;
7:     compute and store $A_q(\zeta_1, \zeta_1), 1 \leq q \leq Q_a$ and $F_q(\zeta_1), 1 \leq q \leq Q_f$;
8:     compute and store $(\mathcal{C}_q, \mathcal{C}_{q'})_X, (\mathcal{C}_q, \mathcal{L}_p^1)_X, (\mathcal{L}_p^1, \mathcal{L}_{p'}^1)_X, 1 \leq q, q' \leq Q_f, 1 \leq p, p' \leq Q_a$;
9:     **for** $N = 2, \ldots, N_{max}$ **do**
10:         compute $\|\hat{e}(y)\|_X^2$ by (3.17) and $\triangle_{N-1}^s(y)$ by (3.12) $\forall y \in \Xi_{train}$;
11:         choose $y^N = \arg\max_{y \in \Xi_{train}} \triangle_{N-1}^s(y)$;
12:         augment the sample space $S_N = S_{N-1} \cup \{y^N\}$;
13:         solve problem (3.2) at y^N to obtain $u(y^N)$;
14:         orthonormalize the solution $u(y^N)$ by Gram-Schmidt process to get ζ_N;
15:         augment the reduced basis space $X_N = X_{N-1} \oplus \text{span}\{\zeta_N\}$;
16:         compute and store $A_q(\zeta_N, \zeta_n), A_q(\zeta_n, \zeta_N), 1 \leq q \leq Q_a, 1 \leq n \leq N$ and $F_q(\zeta_N)$, $1 \leq q \leq Q_f$;
17:         compute and store $(\mathcal{C}_q, \mathcal{C}_{q'})_X, (\mathcal{C}_q, \mathcal{L}_p^N)_X, (\mathcal{L}_p^N, \mathcal{L}_{p'}^N)_X, (\mathcal{L}_p^n, \mathcal{L}_{p'}^N)_X, 1 \leq q, q' \leq Q_f$ $1 \leq p, p' \leq Q_a, 1 \leq n \leq N$;
18:         **if** $\triangle_{N-1}^s(y^N) \leq \varepsilon_{tol}$ **then**
19:             $N_{max} = N$;
20:             **return** ;
21:         **end if**
22:     **end for**
23: **end procedure**

24: **procedure** ONLINE EVALUATION:
25:     given new sample set Ξ_{new}, pre-compute and store $\alpha_{LB}(y), y \in \Xi_{new}$ by SCM [27];
26:     for each $y \in \Xi_{new}$, solve (3.4) to get $u_N(y)$ and compute $s_N(y)$ and $\triangle_N^s(y)$;
27:     evaluate the failure probability by (3.18), where $M = |\Xi_{new}|$.
28: **end procedure**

3.2   Hybrid reduced basis method

As anticipated in section 2.2, Monte Carlo method is an accurate and straightforward approach for evaluation of the failure probability by (2.6), however it is prohibitively expensive as it requires the solution of a large number of PDEs. In contrast, surrogate models built on other methods may improve computational efficiency at the expense of producing incorrect output and thus wrong failure probability estimate. In order to balance the trade-off of computational efficiency and numerical accuracy, a hybrid approach with either direct or iterative algorithms has been developed in [30]. The direct hybrid algorithm predefines a neighborhood region of the critical value by a threshold parameter, then it uses a surrogate model to compute the (surrogate) outputs at samples outside that region and directly solves the PDEs to evaluate the (direct) outputs at samples inside the region. However, the choice of the threshold value depends crucially on the accuracy of the surrogate model, which is not provided in general. On the other hand, the iterative hybrid algorithm replaces some surrogate output closest to the critical value by direct outputs and conduct the replacement iteratively until meeting a posteriori error tolerance. This algorithm does not need to choose the value of a threshold parameter but the accuracy of the failure probability estimate is again affected by the unknown error of the surrogate model. To improve on this, we propose a

hybrid reduced basis method certified by a posteriori error bound, achieving both the computational efficiency and the numerical accuracy.

Since the approximation error of the output at sample y can be bounded by (3.12), we can define the certified surrogate failure domain

$$\Gamma_0^c := \{y \in \Gamma : s_N(y) < s_0, \triangle_N^s(y) < s_0 - s_N(y)\} \tag{3.19}$$

and the uncertified surrogate failure domain

$$\Gamma_0^u := \{y \in \Gamma : \triangle_N^s(y) \geq |s_0 - s_N(y)|\}. \tag{3.20}$$

Whenever the sample y falls in the certified surrogate failure domain Γ_0^c, we have

$$s(y) = (s(y) - s_N(y)) + s_N(y) \leq \triangle_N^s(y) + s_N(y) < s_0 - s_N(y) + s_N(y) = s_0, \tag{3.21}$$

so that any sample $y \in \Gamma_0^c$ also falls in the original failure domain Γ_0. As for the sample in uncertified failure domain $y \in \Gamma_0^u$, we compute a real output $s(y) = s(u(y))$ from the solution $u(y)$ by fully solving the PDE (3.2). Thus, the hybrid failure domain is defined as

$$\Gamma_0^h := \Gamma_0^c \cup (\Gamma_0^u \cap \{y \in \Gamma : s(y) < s_0\}), \tag{3.22}$$

and the hybrid failure probability is evaluated by

$$P_0^h = \frac{1}{M} \sum_{m=1}^{M} \mathcal{X}_{\Gamma_0^h}(y^m). \tag{3.23}$$

By construction, we have that the evaluation of the hybrid failure probability is cheap thanks to the use of the surrogate model and accurate in the sense that it is equal to the Monte Carlo failure probability, $P_0^h = P_0^m$.

In dealing with high dimensional problems, we usually apply an iterative algorithm for Monte Carlo sampling with an increasing number of samples to enhance computational efficiency on the one hand and provide a posteriori error estimate for the Monte Carlo evaluation on the other. The following Algorithm 2 describes the hybrid reduced basis method.

3.3 Goal-oriented adaptive reduced basis method

In order to avoid too many direct solves of the full underlying PDE, we need to increase the portion of the samples in the certified surrogate failure domain, which in turn requires using a more accurate surrogate model constructed with more reduced basis functions. However, the computational cost of both the offline construction and the online evaluation of reduced basis method depends critically on the number of reduced basis functions, suggesting therefore the use of a low number of reduced basis functions, especially for high dimensional problems. In addition, when the surrogate output is far from the critical value, a rather crude surrogate approximation with a small number of reduced basis functions would be sufficient as long as the a posteriori error bound for the approximation error of the output is smaller than the distance between the surrogate output and the critical value. To take full advantage of the reduced basis approximation and a posteriori error bound, we develop a goal-oriented adaptive strategy to construct a surrogate model with fine approximation of the output manifold close to the limit state surface $\{y \in \Gamma : s(y) = s_0\}$ and coarse approximation of the output manifold far away from it.

Goal-oriented adaptive strategies have been developed in many contexts (e.g. [39, 40]). For its application in the construction of surrogate model, we first run the Algorithm 1 for reduced basis method with a relatively small training set Ξ_{train} and large tolerance ε_{tol} as stopping criteria. Given any new sample set Ξ_M with M samples, we compute the surrogate outputs s_N and the

---

Algorithm 2 Iterative algorithm for hybrid reduced basis method

---

1: **procedure** OFFLINE CONSTRUCTION:
2:     Construct a reduced basis space X_N by Algorithm 1.
3: **end procedure**

4: Initialize tolerance ϵ_{tol} and a posteriori error $e_1^p = 2\epsilon_{tol}$, choose the number of initial samples M, adaptive size parameter β as well as a maximum iteration number I_{max};
5: **procedure** ITERATIVE EVALUATION:
6:     **for** $i = 1, \ldots, I_{max}$ **do**
7:         sample Ξ_M with $|\Xi_M| = M$, pre-compute and store $\alpha_{LB}(y), y \in \Xi_M$ by SCM [27];
8:         compute surrogate output $s_N(y)$ and the error bound $\triangle_N^s(y)$ by (3.12) for $\forall y \in \Xi_M$;
9:         evaluation the failure probability $P_0^{h,i}$ by formula (3.23);
10:         **if** $i > 1$ **then**
11:             compute the a posteriori error for failure probability $e_i^p = |P_0^{h,i} - P_0^{h,i-1}|$;
12:             **if** $e_i^p < \epsilon_{tol}$ **then**
13:                 $I_{max} = i$;
14:                 **return** ;
15:             **end if**
16:         **end if**
17:         increase the number of sample size by setting $M = \beta^{i+1}M$;
18:     **end for**
19: **end procedure**

---

associated error bounds $\triangle_N^s$, from which we define the following adaptive criteria

$$\triangle_N^a(y) = \frac{\triangle_N^s(y)}{|s_N(y) - s_0|} \quad \forall y \in \Xi_M. \tag{3.24}$$

We apply again the greedy algorithm to select the most mismatching sample

$$y^{N+1} = \arg \min_{y \in \Xi_M} \triangle_N^a(y) \text{ such that } \triangle_N^a(y^{N+1}) \geq 1, \tag{3.25}$$

and enrich the reduced basis space by $X_{N+1} = X_N \oplus \text{span}\{\zeta^{N+1}\}$ where ζ^{N+1} is the orthonormalized version of the solution $u(y^{N+1})$ of problem (3.2). We carry out the sample procedure of reduced basis construction with $N = N + 1$ until $\triangle_N^a(y^{N+1}) < 1$. Then we compute the failure probability by formula (3.18), which is accurate since $\triangle_N^s(y) < |s_N(y) - s_0| \forall y \in \Xi_M$ and thus the certified surrogate failure domain Γ_0^c is the real failure domain Γ_0.

    Algorithm 3 combines the goal-oriented adaptive strategy with the iterative scheme for Monte Carlo evaluation of failure probability. As a profit of the adaptive construction of the reduced basis space, the failure probability is computed asymptotically based on a posteriori error in Algorithm 2 and 3. In order to further quantify the precision of the failure probability, one may also provide the binomial confidence interval for the failure probability [52], e.g. the normal approximation interval $P_0 \pm z_{1-\alpha_e/2}\sqrt{P_0(1-P_0)/M}$, being P_0 the failure probability computed by either the hybrid or the adaptive algorithm with M Monte Carlo samples, $z_{1-\alpha_e/2}$ a percentile of a standard normal distribution and α_e a prescribed error percentile.

3.4   Remarks on approximation error and computational cost

The approximation error of the failure probability by the three different approaches described above can be generally split into the one arising from the surrogate models and the other from Monte Carlo method. In the first approach (described in section 3.1), the approximation error of the surrogate model may lead to a large error or even wrong evaluation of the failure probability due to the discontinuous or singular properties of the limit state surface, while in the last two approaches (described in section 3.2 and 3.3), the contribution of the approximation error from

---

Algorithm 3 Iterative algorithm for goal-oriented adaptive reduced basis method

---

1: **procedure** OFFLINE CONSTRUCTION:
2:     Construct a crude reduced basis space X_N by Algorithm 1.
3: **end procedure**

4: Initialize tolerance ϵ_{tol} and a posteriori error $e_1^p = 2\epsilon_{tol}$, choose the number of initial samples M, adaptive size parameter β as well as a maximum iteration number I_{max};
5: **procedure** ADAPTIVE CONSTRUCTION:
6:     **for** $i = 1, \ldots, I_{max}$ **do**
7:         sample Ξ_M with $|\Xi_M| = M$, pre-compute and store $\alpha_{LB}(y), y \in \Xi_M$ by SCM [27];
8:         compute surrogate outputs $s_N(y)$ and adaptive criteria $\triangle_N^a(y)$ by (3.24) for $\forall y \in \Xi_M$;
9:         choose adaptive sample $y^{N+1} = \arg\max_{y \in \Xi_M} \triangle_N^a(y)$;
10:        **while** $\triangle_N^a(y^{N+1}) \geq 1$ **do**
11:            augment the sample space $S_{N+1} = S_N \cup \{y^{N+1}\}$;
12:            solve problem (3.2) at y^{N+1} to obtain $u(y^{N+1})$;
13:            orthonormalize the solution $u(y^{N+1})$ by Gram-Schmidt process to get ζ_{N+1};
14:            augment the reduced basis space $X_{N+1} = X_N \oplus \text{span}\{\zeta_{N+1}\}$;
15:            compute and store $A_q(\zeta_{N+1}, \zeta_n), A_q(\zeta_n, \zeta_{N+1}), 1 \leq q \leq Q_a, 1 \leq n \leq N+1$ and $F_q(\zeta_{N+1}), 1 \leq q \leq Q_f$;
16:            compute and store $(\mathcal{C}_q, \mathcal{C}_{q'})_X, (\mathcal{C}_q, \mathcal{L}_p^{N+1})_X, (\mathcal{L}_p^{N+1}, \mathcal{L}_{p'}^n)_X, (\mathcal{L}_p^n, \mathcal{L}_{p'}^{N+1})_X$, $1 \leq q, q' \leq Q_f, 1 \leq p, p' \leq Q_a, 1 \leq n \leq N+1$;
17:            set N = N + 1;
18:            compute $s_N(y)$ and $\triangle_N^a(y)$ by (3.24) $\forall y \in \Xi_M$;
19:            choose adaptive sample $y^{N+1} = \arg\max_{y \in \Xi_M} \triangle_N^a(y)$;
20:        **end while**
21:        evaluation the failure probability $P_0^{s,i}$ by formula (3.18);
22:        **if** $i > 1$ **then**
23:            compute the a posteriori error for failure probability $e_i^p = |P_0^{s,i} - P_0^{s,i-1}|$;
24:            **if** $e_i^p < \epsilon_{tol}$ **then**
25:                $I_{max} = i$;
26:                **return** ;
27:            **end if**
28:        **end if**
29:        increase the number of sample size by setting $M = \beta^{i+1}M$;
30:    **end for**
31: **end procedure**

---

surrogate models is null and the Monte Carlo approximation error takes full responsibility with a slow algebraic decaying rate $M^{-1/2}$.

As for computational cost, the first approach is the cheapest one as it does not necessitate to solve a full PDE in the evaluation procedure once the offline construction is finished. In contrast, the hybrid approach is relatively expensive, as it requires to solve the full PDE whenever the a posteriori error bound is larger than the distance between the surrogate output and the critical value. The goal-oriented adaptive approach is much cheaper than the hybrid one since it starts from a rather crude reduced basis construction and replaces many direct outputs in the hybrid approach by surrogate outputs based on adaptively enriched reduced basis space. Moreover, it might be even cheaper than the first approach if its total offline construction is less expensive than that of the first approach.

4   Extension to more general PDE models

The development of both hybrid and goal-oriented adaptive reduced basis methods is based on the benchmark linear elliptic PDE with random inputs (2.1), which is assumed to be compliant

in the output, time independent, affine in the random inputs and coercive. In this section, we remove these limitations and extend the proposed methods to more general PDE models. The key elements in the extension are to accurately compute cheap, reliable and sharp a posteriori error bound for the approximation error of the output and efficiently decompose the approximation procedure into the offline construction stage and the online evaluation stage. We remark that most of the techniques we are using have been well studied for the development and application of reduced basis method [44], and we briefly summarize them with specific application in the context of failure probability computation. In addition, most of the proposed algorithms can be extended to the case of multiple functional outputs of the solution field. In fact, for a small number of independent functional outputs, we may treat each of them separately as in the case of a single functional output. When there are many coupled functional outputs, a common coarse reduced basis space is more convenient to be used in combination with suitable refinement with respect to each functional output in order to keep the total computational cost under control.

4.1 Non-compliant problems

When the output is compliant, i.e. $s(y) \equiv s(u(y); y) = F(u(y); y), y \in \Gamma$, as presented in section 3.1.2, we obtain a posteriori error bound $\triangle_N^s(y)$ being quadratic with respect to the residual norm $||\hat{e}(y)||_X$. However, when the output is non-compliant in more general conditions, i.e.

$$s(y) \equiv s(u(y); y) = L(u(y); y), \tag{4.1}$$

where $L : X \to \mathbb{R}$ is a bounded and affine functional, $L \neq F$, we have the following upper bound

$$|s(y) - s_N(y)| \leq ||L(y)||_{X'}||u(y) - u_N(y)||_X \leq \frac{1}{\alpha(y)}||L(y)||_{X'}||\hat{e}(y)||_X, \tag{4.2}$$

which depends only linearly on the residual norm $||\hat{e}(y)||_X$. Moreover, evaluation of the dual norm of the functional $||L(y)||_{X'}$ is expensive and might not be uniformly bounded in the probability domain Γ. In order to seek an effective and efficient a posteriori error bound for the output approximation error, we apply the primal-dual computational strategy [50, 41, 44] by solving an additional problem, known as the dual problem associated to the functional L: $\forall y \in \Gamma$ find the dual variable $\psi(y) \in X$ such that

$$A(v, \psi(y); y) = -L(v; y) \quad \forall v \in X. \tag{4.3}$$

By the same reduced basis approximation procedure as in section 3.1, we construct the reduced basis space for the approximation of the dual variable ψ as $X_{N_{du}}^{du} := \text{span}\{\zeta_1^{du}, \ldots, \zeta_{N_{du}}^{du}\}$ where $\zeta_n^{du}, 1 \leq n, \leq N_{du}$ are determined via orthonormalization from the solution $\{\psi(y^n), 1 \leq n \leq N_{du}\}$ (at suitable values of $y^n, 1 \leq n \leq N_{du}$), then the reduced basis solution $\psi_{N_{du}}(y)$ at sample $y \in \Gamma$ is obtained by solving the reduced system

$$A(v, \psi_{N_{du}}(y); y) = -L(v; y) \quad \forall v \in X_{N_{du}}^{du}. \tag{4.4}$$

Let us denote the primal reduced basis space as $X_{N_{pr}}^{pr} := \text{span}\{\zeta_1^{pr}, \ldots, \zeta_{N_{pr}}^{pr}\}$ and rewrite the reduced system for the primal reduced basis solution $u_{N_{pr}}$ as

$$A(u_{N_{pr}}(y), v; y) = F(v; y) \quad \forall v \in X_{N_{pr}}^{pr}. \tag{4.5}$$

Furthermore, let us define the primal residual and dual residual respectively as

$$R^{pr}(v; y) = F(v; y) - A(u_{N_{pr}}(y), v; y) \quad \text{and} \quad R^{du}(v; y) = -L(v; y) - A(v, \psi_{N_{du}}(y); y). \tag{4.6}$$

By solving the primal and dual reduced system, we can evaluate the non-compliant output by

$$s_N(y) = L(u_{N_{pr}}(y)) - R^{pr}(\psi_{N_{du}}(y); y). \tag{4.7}$$

The following lemma provides an efficient a posteriori error bound for the output [50, 41, 44].

Lemma 4.1 *The approximation error on the output $|s(y) - s_N(y)|$ is bounded from above by the following a posteriori error bound $\triangle_N^s(y)$*

$$|s(y) - s_N(y)| \leq \triangle_N^s(y) := \frac{||R^{pr}(\cdot; y)||_{X'} ||R^{du}(\cdot; y)||_{X'}}{\alpha_{LB}(y)} \quad \forall y \in \Gamma, \tag{4.8}$$

where $||R^{pr}(\cdot; y)||_{X'}$ and $||R^{du}(\cdot; y)||_{X'}$ are the dual norms of the primal and dual residuals.

Remark 4.1 *Besides converging faster, the primal-dual computational strategy does not require the computation of the dual norm $||L(y)||_{X'}, \forall y \in \Gamma$. On their turn, the dual norms $||R^{pr}(\cdot; y)||_{X'}$ and $||R^{du}(\cdot; y)||_{X'}$ can be efficiently evaluated by the offline-online computational decomposition as presented in section 3.1.3.*

As for the evaluation of failure probability in non-compliant problems, the reduced basis method in Algorithm 1 remains the same as in the compliant case, and the hybrid reduced basis method in Algorithm 2 is essentially the same as in compliant problems except for the replacement of a posteriori error bound (4.8). In the goal-oriented adaptive Algorithm 3, we enrich simultaneously both the primal and the dual reduced basis spaces governed by the posteriori error bound (4.8) in order to gain more computational efficiency for the evaluation of failure probability in non-compliant problems.

4.2 Non-steady problems

If the state variable depends not only on the spatial variable $x \in D$ but also the temporal variable $t \in I \equiv [0, T]$, we have to face a non-steady PDE; a suitable time discretization needs to be taken into account for both the offline construction of reduced basis space and the online evaluation of the output. For the sake of simplicity [25, 44], we consider the following parabolic problem in semi-weak formulation: find $u(y) \in L^2(I; X) \cap C^0(I; L^2(D))$ such that it holds, almost surely

$$M\left(\frac{\partial u}{\partial t}(t; y), v; y\right) + A(u(t; y), v; y) = g(t)F(v; y) \quad \forall v \in X, \tag{4.9}$$

subject to initial condition $u(0; y) = u_0 \in L^2(D)$. Here, $g \in L^2(I)$ is a time dependent control function; X is a spatial approximation space as defined in section 3.1, e.g. finite element space; the bilinear form A and linear form F are defined as in the elliptic problem, and the bilinear form M is assumed to be uniformly continuous and coercive and featuring the following affine expansion

$$M(w, v; y) = \sum_{q=1}^{Q_m} \Theta_q^m(y) M_q(w, v) \quad \forall w, v \in X. \tag{4.10}$$

Using (without loss of generality) the backward Euler scheme for time discretization, we find at every time step

$$M(u^i(y), v; y) + \triangle t A(u^i(y), v; y) = \triangle t g(t^i) F(v; y) + M\left(u^{i-1}(y), v; y\right) \quad \forall v \in X, \tag{4.11}$$

subject to the initial condition $u(t^0; y) = u_0$, where $\triangle t$ is the time step size, $u^i(y) \simeq u(t^i; y), 0 \leq i \leq I_T \equiv T/\triangle t$. We remark that we don't take into account the time discretization error for the sake of simplicity. We consider a compliant output $s(t^i; y) = F(u^i(y); y), 1 \leq i \leq I_T, y \in \Gamma$. As for

non-compliant output, we apply the primal-dual computational strategy presented in section 4.1, see non-steady problems with more general outputs in [25, 48]. A reduced problem associated to (4.11) can be formulated as: find $u_N^i(y) \in X_N, 1 \leq i \leq I_T$ such that

$$M(u_N^i(y), v; y) + \triangle t A(u_N^i(y), v; y) = \triangle t g(t^i) F(v; y) + M\left(u_N^{i-1}(y), v; y\right) \quad \forall v \in X_N, \qquad (4.12)$$

where the reduced basis space X_N can be constructed by a POD-greedy sampling algorithm governed by cheap a posteriori error bound as well as an efficient offline-online computational decomposition procedure, which are presented in the following subsections respectively.

4.2.1 A POD-greedy algorithm

In non-steady problems, the samples for the construction of the reduced basis space involve not only the random samples $y \in \Xi_{train} \subset \mathbb{R}^K$ in multiple dimensions but also the temporal samples $t^i \in I \subset \mathbb{R}, 1 \leq i \leq I_T$ in one dimension. A pure greedy sampling algorithm in both probability space and temporal space has been demonstrated inefficient and resulting in occasional infinite loop [26]. A POD-greedy algorithm, based on POD selection in temporal space and greedy selection in probability space, has been effectively used in [26] for tackling these difficulties. A general formulation for POD is stated as follows: given a training set X_{train} with n_{train} elements, the function $X_M = \text{POD}(X_{train}, M)$ leads to an optimal subset $X_M \subset \text{span}\{X_{train}\}$ with M bases such that

$$X_M = \arg \inf_{Y_M \subset \text{span}\{X_{train}\}} \left(\frac{1}{n_{train}} \sum_{v \in X_{train}} \inf_{w \in Y_M} ||v - w||_X^2 \right)^{1/2}. \qquad (4.13)$$

In practice, we solve the eigenvalue problem $C\zeta = \lambda\zeta$, where the correlation matrix C is assembled by the weighted correlation of the elements $v_n \in X_{train}, 1 \leq n \leq n_{train}$ as

$$C_{mn} = \frac{1}{n_{train}}(v_m, v_n)_X, 1 \leq m, n \leq n_{train}, \qquad (4.14)$$

and the subset $X_M = \text{span}\{\zeta_m, 1 \leq m \leq M\}$ where $\zeta_m, 1 \leq m \leq M$ are the orthonormal eigenfunctions corresponding to the M largest eigenvalues. Provided a tolerance ε_{pod} is given, we can also redefine the function $X_M = \text{POD}(X_{train}, \varepsilon_{pod})$ such that the sum of $n_{train} - M$ smallest eigenvalues is smaller than ε_{tol}. The POD-greedy algorithm for the construction of reduced basis space in non-steady problems is presented in Algorithm 4 [44, 26].

Algorithm 4 A POD-greedy algorithm

1: Initialize a random sample $y^* \in \Xi_{train}$, the tolerances ε_{tol} and ε_{pod}, an empty reduced basis space Y as well as a maximum number of reduced basis functions N_{max}, set $N = 0$;
2: **procedure** ITERATIVE CONSTRUCTION:
3:     **while** $N \leq N_{max}$ **do**
4:         solve the parabolic problem (4.11) at sample y^* and time $t^i, 1 \leq i \leq I_t$;
5:         compute $X_{M_1} = \text{POD}(\{u^i(y^*), 1 \leq i \leq I_t\}, \varepsilon_{pod})$;
6:         enrich the reduced basis space $Y = Y \cup X_{M_1}$;
7:         update the number of reduced basis functions $N = N + M_2$, where $M_2 \leq M_1$;
8:         construct the reduced basis space $X_N = \text{POD}(Y, N)$;
9:         choose sample $y^* = \arg \max_{y \in \Xi_{train}} \triangle_N^s(T; y)$ by greedy algorithm;
10:         **if** $\triangle_N^s(T; y^*) \leq \varepsilon_{tol}$ **then**
11:             $N_{max} = N$;
12:             **return** ;
13:         **end if**
14:     **end while**
15: **end procedure**

We remark that in Algorithm 4 the step integer M_1 is controlled by the tolerance of the

internal POD algorithm, offering flexibility in choosing the number of reduced basis functions from the elements $u^i(y^*), 1 \leq i \leq I_t$, and M_2 is chosen to be smaller than M_1 in order to minimize duplication of the reduced basis functions. The random sample y^*, which might be the same in different iteration steps, is chosen by greedy algorithm governed by cheap and sharp a posteriori error bound $\triangle_N^s(T; y), y \in \Gamma$ constructed in the following sections.

4.2.2 Construction of a posteriori error bound

We follow the procedure in section 3.1.2 to briefly introduce how to construct a posteriori error bound for the parabolic problem (4.11). Firstly, we define the reduced residual for $1 \leq i \leq I_t$,

$$R^i(v; y) = g(t^i)F(v; y) - \frac{1}{\triangle t}M(u_N^i(y) - u_N^{i-1}(y), v; y) - A(u_N^i(y), v; y) \quad \forall v \in X_N. \qquad (4.15)$$

By Riesz representation theorem [18], we have a unique function $\hat{e}^i(y) \in X, 1 \leq i \leq I_t$ such that $(\hat{e}^i(y), v)_X = R^i(v; y)$ and $||\hat{e}^i(y)||_X = ||R^i(\cdot; y)||_{X'}, 1 \leq i \leq I_t$. Furthermore, it can be proven that the reduced basis approximation error for the output is bounded by [25]

$$|s(t^i; y) - s_N(t^i; y)| \leq \triangle_N^s(t^i; y) := \frac{1}{\alpha_{LB}(y)} \sum_{i'=1}^{i} ||\hat{e}^{i'}(y)||_X^2, 1 \leq i \leq I_t. \qquad (4.16)$$

4.2.3 Offline-online computational decomposition

By expansion of the reduced basis solution at time $t^i, 1 \leq i \leq I_t$ in the reduced basis functions

$$u_N^i(y) = \sum_{m=1}^{N} u_{Nm}^i(y)\zeta_m, \qquad (4.17)$$

we have the reduced basis problem by Galerkin projection in (4.11) as: find $u_{Nm}^i(y), 1 \leq m \leq N, 1 \leq i \leq I_t$ such that

$$\sum_{m=1}^{N}\sum_{q=1}^{Q_m}\Theta_q^m(y)M_q(\zeta_m, \zeta_n)u_{Nm}^i(y) + \triangle t \sum_{m=1}^{N}\sum_{q=1}^{Q_a}\Theta_q^a(y)A_q(\zeta_m, \zeta_n)u_{Nm}^i(y)$$
$$= \triangle t g(t^i)\sum_{q=1}^{Q_f}\Theta_q^f(y)F_q(\zeta_n) + \sum_{m=1}^{N}\sum_{q=1}^{Q_m}\Theta_q^m(y)M_q(\zeta_m, \zeta_n)u_{Nm}^{i-1}(y) \quad 1 \leq n \leq N, \qquad (4.18)$$

where the matrices $M_q(\zeta_m, \zeta_n), 1 \leq q \leq Q_m, 1 \leq m, n \leq N$, $A_q(\zeta_m, \zeta_n), 1 \leq q \leq Q_a, 1 \leq m, n \leq N$ and the vectors $F_q(\zeta_n), 1 \leq q \leq Q_f, 1 \leq n \leq N$ can be pre-computed and stored in the offline construction stage. In the online evaluation stage, we only need to assemble and solve a $N \times N$ system (4.18) to get the solution $u_N^i(y)$ and evaluate the output by NQ_f operations

$$s_N(t^i; y) = F(u_N^i(y); y) = \sum_{n=1}^{N}\left(\sum_{q=1}^{Q_f}\Theta_q^f(y)F_q(\zeta_n)\right)u_{Nn}^i(y). \qquad (4.19)$$

As for the evaluation of the error bound (4.16), we substitute the reduced basis solution (4.17) in the residual (4.15) and compute the residual norm $||\hat{e}^i(y)||_X$ by assembling

$$
\begin{aligned}
||\hat{e}^i(y)||_X^2 = {} & g^2(t^i) \sum_{q}^{Q_f} \sum_{q'}^{Q_f} \Theta_q^f(y) \Theta_{q'}^f(y) (\mathcal{C}_q, \mathcal{C}_{q'})_X \\
& + 2\frac{g(t^i)}{\triangle t} \sum_{n=1}^{N} \sum_{q=1}^{Q_f} \sum_{q'=1}^{Q_m} \Theta_q^f(y) \Theta_{q'}^m(y) (\mathcal{C}_q, \mathcal{M}_{q'}^n)_X \varphi_{Nn}^i(y) \\
& + 2g(t^i) \sum_{n=1}^{N} \sum_{q=1}^{Q_f} \sum_{q'=1}^{Q_a} \Theta_q^f(y) \Theta_{q'}^a(y) (\mathcal{C}_q, \mathcal{L}_{q'}^n)_X u_{Nn}^i(y) \\
& + \frac{1}{\triangle t^2} \sum_{n=1}^{N} \sum_{n'=1}^{N} \sum_{q=1}^{Q_m} \sum_{q'=1}^{Q_m} \Theta_q^m(y) \Theta_{q'}^m(y) \varphi_{Nn}^i(y) (\mathcal{M}_q^n, \mathcal{M}_{q'}^{n'})_X \varphi_{Nn'}^i(y) \\
& + 2\frac{1}{\triangle t} \sum_{n=1}^{N} \sum_{n'=1}^{N} \sum_{q=1}^{Q_m} \sum_{q'=1}^{Q_a} \Theta_q^m(y) \Theta_{q'}^a(y) \varphi_{Nn}^i(y) (\mathcal{M}_q^n, \mathcal{L}_{q'}^{n'})_X u_{Nn'}^i(y) \\
& + \sum_{n=1}^{N} \sum_{n'=1}^{N} \sum_{q=1}^{Q_a} \sum_{q'=1}^{Q_a} \Theta_q^a(y) \Theta_{q'}^a(y) u_{Nn}^i(y) (\mathcal{L}_q^n, \mathcal{L}_{q'}^{n'})_X u_{Nn'}^i(y),
\end{aligned}
\tag{4.20}
$$

where $\varphi_{Nn}^i(y) = u_{Nn}^i(y) - u_{Nn}^{i-1}(y)$, $\mathcal{C}_q, 1 \leq q \leq Q_f$ and $\mathcal{L}_q^n, 1 \leq q \leq Q_a, 1 \leq n \leq N$ are defined as in the elliptic case in section 3.1.3, and $\mathcal{M}_q^n, 1 \leq q \leq Q_m, 1 \leq n \leq N$ are defined such that $(\mathcal{M}_q^n, v)_X = -M_q(\zeta_n, v), \forall v \in X$, which are pre-computed and stored in the offline stage. In the online stage, we only need to assemble (4.20) by $O((Q_f + NQ_m + NQ_a)^2)$ operations, which is very efficient because the values $Q_f, Q_m, Q_a, N \ll \mathcal{N}$ are small.

Methods for the evaluation of failure probability in non-steady problems is not different than those used in the elliptic problems. In particular, we can use the same goal-oriented adaptive procedure 3 with the POD-greedy sampling Algorithm 4 governed by the a posterior error bound (4.16).

4.3 Non-affine problems

The affine assumption made in (3.1) is crucial for an effective offline-online computational decomposition. In the case of a more general non-affine random field denoted by $g(x, y)$, we seek a computational method to approximately decompose the random field $g(x, y)$ in finite affine terms, written as

$$
g(x, y) \approx \mathcal{I}_Q[g](x, y) = \sum_{q=1}^{Q} \Theta_q(y) g_j(x).
\tag{4.21}
$$

4.3.1 Empirical interpolation method

Among many possible affine approximation schemes, e.g. Lagrange interpolation at different points, Fourier expansion on various bases, etc., an empirical interpolation procedure [4, 11] has been developed and extensively used as a very efficient approach in the context of reduced basis method. In principle, it shares similar idea as reduced basis approximation by constructing the affine decomposition in a greedy way governed by a posteriori error. An empirical interpolation for affine decomposition is presented in the following Algorithm 5 [4, 11].

We remark that the nodes in the vertex set V_x are chosen as the discretization nodes in the deterministic approximation method, e.g. finite element nodes. The $L^\infty(V_x)$ optimization problem (4.22) is solved by a linear programming procedure [4], which is expensive if the cardinalities $|V_x|, |\Xi_y|$ are large. In practice, we can replace (4.22) by a cheaper $L^2(V_x)$ optimization problem [24] or the following optimization problem with residual as surrogate a posteriori error for further

---

Algorithm 5 An empirical interpolation for affine decomposition

---

1: **procedure** OFFLINE CONSTRUCTION:
2:     Given function $g \in C^0(\Gamma; L^\infty(D))$, we choose finite set $\Xi_y \subset \Gamma$ and $V_x \subset D$;
3:     find $y^1 = \arg\max_{y \in \Xi_y}(\operatorname{ess\,sup}_{x \in V_x} |g(x,y)|)$ and $x^1 = \arg \operatorname{ess\,sup}_{x \in V_x} |g(x,y^1)|$;
4:     define $r_1 = g$, set the first affine basis $g_1(x) = r_1(x,y^1)/r_1(x^1, y^1)$,
5:     set $Q = 1, Q_{max}$, specify tolerance ε_{tol}, build $W_1 = \operatorname{span}\{g(x,y^1)\}$;
6:     **while** $Q < Q_{max}$ & $r_Q(x^Q, y^Q) > \varepsilon_{tol}$ **do**
7:         find $y^{Q+1} \in \Xi_y$ such that

$$y^{Q+1} = \arg\max_{y \in \Xi_y} \left(\inf_{h \in W_Q} ||g(y) - h||_{L^\infty(V_x)} \right); \tag{4.22}$$

8:         find $\Theta(y^{Q+1}) = (\Theta_1(y^{Q+1}), \ldots, \Theta_Q(y^{Q+1}))^T$ by solving

$$\sum_{q=1}^{Q} \Theta_q(y^{Q+1}) g_q(x^i) = g(x^i, y^{Q+1}) \quad 1 \le i \le Q; \tag{4.23}$$

9:         define $r_{Q+1} : D \times \Gamma \to \mathbb{R}$ as

$$r_{Q+1}(x,y) = g(x,y) - \sum_{q=1}^{Q} \Theta_q(y) g_q(x); \tag{4.24}$$

10:         find $x^{Q+1} \in V_x$ such that

$$x^{Q+1} = \arg \operatorname{ess\,sup}_{x \in V_x} |r_{Q+1}(x, y^{Q+1})|; \tag{4.25}$$

11:         define $g_{Q+1} : D \to \mathbb{R}$ as

$$g_{Q+1}(x) = \frac{r_{Q+1}(x, y^{Q+1})}{r_{Q+1}(x^{Q+1}, y^{Q+1})}; \tag{4.26}$$

12:         update $W_{Q+1} = \operatorname{span}\{g(x, y^i), 1 \le i \le Q+1\}$ and set $Q = Q + 1$.
13:     **end while**
14: **end procedure**

15: **procedure** ONLINE EVALUATION:
16:     For $\forall y \in \Gamma$, construct (4.21) by solving (4.23) with $y^{Q+1} = y$.
17: **end procedure**

---

computational efficiency [31, 11]:

$$y^{Q+1} = \arg\max_{y \in \Xi_y} \left(\operatorname{ess\,sup}_{x \in V_x} |r_{Q+1}(x,y)| \right). \tag{4.27}$$

It has been proven in [11] that the empirical interpolation Algorithm 5 achieves quasi-optimal affine approximation with an error bound presented in the following proposition.

Proposition 4.2 *The empirical interpolation approximation error can be bounded by*

$$||g(y) - \mathcal{I}_Q[g](y)||_{L^\infty(V_x)} \le (Q+1) 2^Q d_Q(L^\infty(V_x); y), \tag{4.28}$$

where d_Q is the Kolmogorov width [6] quantifying the optimal approximation error by any possible

Q dimensional subspace H_Q of a Hilbert space $\mathcal{H}$, defined as

$$d_Q(\mathcal{H}; y) := \inf_{H_Q} \sup_{g(y) \in \mathcal{H}} \inf_{h \in H_Q} ||g(y) - h||_{\mathcal{H}}. \qquad (4.29)$$

Remark 4.2 *Proposition 4.2 states that the empirical interpolation error can not be worse than the best possible approximation error upon multiplication by a factor $(Q+1)2^Q$. Specifically, when $d_Q \le ce^{-rQ}$ with $r > \log(2)$, we have the following a priori error estimate with exponential decay*

$$||g - \mathcal{I}_Q[g]||_{L^\infty(V_x)} \le ce^{-(r - \log(2))Q}. \qquad (4.30)$$

4.3.2 Global a posteriori error estimate

Let us now extend the affine assumption (3.1) to more general non-affine random fields for both the diffusion coefficient a and the force term f in (2.1). By empirical interpolation, we obtain the following affine decomposition

$$a \approx a_{Q_a} \equiv \mathcal{I}_{Q_a}[a] = \sum_{q=1}^{Q_a} \Theta_q^a(y) a_q(x) \text{ and } f \approx f_{Q_f} \equiv \mathcal{I}_{Q_f}[f] = \sum_{q=1}^{Q_f} \Theta_q^f(y) f_q(x). \qquad (4.31)$$

For the reduced basis approximation with affine decomposition of the non-affine random inputs, we state the following two lemmas for global a posteriori reduced basis approximation error estimate of the solution and the output. The proofs are deferred to the Appendix.

Lemma 4.3 *Suppose the approximation by affine decomposition (4.31) results in an approximate solution u_Q of problem (3.2) and a reduced basis solution $u_{Q,N}$ of (3.4). The following a posteriori error bound for the reduced basis approximation error holds*

$$||u(y) - u_{Q,N}(y)||_X \le \mathcal{E}_Q^u(y) + \triangle_N^u(y), \qquad (4.32)$$

where $\triangle_N^u$ is a posteriori error bound for the reduced basis approximation defined in (3.11), $\mathcal{E}_Q$ the error due to the affine approximation of the data a and f, defined as

$$\mathcal{E}_Q^u(y) := \frac{C_1}{\alpha_{LB}(y)} ||f(y) - f_{Q_f}(y)||_{L^\infty(D)} + \frac{C_1 C_2}{\alpha_{LB}^2(y)} ||a(y) - a_{Q_a}(y)||_{L^\infty(D)} ||f_{Q_f}(y)||_{L^\infty(D)}, \qquad (4.33)$$

C_1, C_2 two constants bounded by (A.18) and $\alpha_{LB}(y), y \in \Gamma$ a lower bound of the coercivity constant of the bilinear form (A.4) with respect to the norm $|| \cdot ||_X$.

Lemma 4.4 *As for the approximation error between the compliant output $s(y) = (f(y), u(y))$ and the approximate compliant output $s_{Q,N}(y) = (f_{Q_f}(y), u_{Q,N}(y))$, we have*

$$|s(y) - s_{Q,N}(y)| \le \mathcal{E}_Q^s(y) + \triangle_N^s(y), \qquad (4.34)$$

where $\triangle_N^s$ is a posteriori error bound for the reduced basis approximation corresponding to (3.12), $\mathcal{E}_Q^s$ is the error due to the affine approximation of data a and f, defined as

$$\mathcal{E}_Q^s(y) := \frac{C_1^2}{\alpha_{LB}(y)} ||f(y) - f_{Q_f}(y)||_{L^\infty(D)} ||f_{Q_f}(y)||_{L^\infty(D)} + C_1 ||f(y)||_{L^\infty(D)} \mathcal{E}_Q^u(y), \qquad (4.35)$$

where the constant C_1, the lower bound $\alpha_{LB}(y)$ and $\mathcal{E}_Q^u(y), y \in \Gamma$, are defined in Lemma 4.3.

Remark 4.3 *As a result of Lemma 4.3 and Lemma 4.4, the approximation error for both the solution and the output can be decomposed into two components: one arising from the empirical interpolation error of the random fields and another from the reduced basis approximation error. Unfortunately, the evaluation of the empirical interpolation error for each sample $y \in \Gamma$ in (4.33) and (4.35) involves computing $|| \cdot ||_{L^\infty(D)}$ norm with at least $O(\mathcal{N})$ operations, being $\mathcal{N} = |V_x|$ the number of the finite element nodes. This would spoil the cheap online evaluation cost for a large number of samples required in the computation of failure probability, especially when $\mathcal{N}$ becomes very large.*

4.3.3   Cheap a posteriori error bound

To overcome the drawback of computational inefficiency pointed out in Remark 4.3, we seek the upper bounds $\mathcal{E}_Q^{u,b}$ and $\mathcal{E}_Q^{s,b}$ for the affine approximation error of the solution $\mathcal{E}_Q^u \leq \mathcal{E}_Q^{u,b}$ and the output $\mathcal{E}_Q^s \leq \mathcal{E}_Q^{s,b}$, whose computational cost is small and independent of $\mathcal{N}$.

By the empirical interpolation Algorithm 5, we obtain from (4.25) and (4.27) the error bound

$$||a(y) - a_{Q_a}(y)||_{L^\infty(D)} \leq r_{Q_a+1}^a(x^{Q_a+1}, y^{Q_a+1}) \quad \forall y \in \Xi_y^a \tag{4.36}$$

and

$$||f(y) - f_{Q_f}(y)||_{L^\infty(D)} \leq r_{Q_f+1}^f(x^{Q_f+1}, y^{Q_f+1}) \quad \forall y \in \Xi_y^f, \tag{4.37}$$

where $r_{Q_a+1}^a$ and $r_{Q_f+1}^f$ are the the empirical interpolation errors defined in (4.24) corresponding to the non-affine random fields a and f, respectively. Although the relation (4.36) and (4.37) hold true only in the sample sets Ξ_y^a and Ξ_y^f, we remark that in practice they also often hold in the whole probability domain Γ, especially when the cardinality of sample sets is big or the random fields are rather smooth with respect to the random vector y.

Since computing $||f_{Q_f}(y)||_{L^\infty(D)}$ in (4.33) and (4.35) for $y \in \Gamma$ is expensive, we bound the quantity $||u_Q(y)||_X$ in (A.13) directly by

$$||u_Q(y)||_X \leq ||u_{Q,N}(y)||_X + \triangle_N^u(y), \tag{4.38}$$

(instead than by (A.14)), which can be cheaply evaluated in the online stage. Now we can compute the following error bound for the affine approximation error of the solution by using (4.36), (4.37) and (4.38),

$$\begin{aligned}\mathcal{E}_Q^{u,b}(y) := & \frac{C_1}{\alpha_{LB}(y)} r_{Q_f+1}^f(x^{Q_f+1}, y^{Q_f+1}) \\ & + \frac{C_2}{\alpha_{LB}(y)} r_{Q_a+1}^a(x^{Q_a+1}, y^{Q_a+1})(||u_{Q,N}(y)||_X + \triangle_N^u(y)).\end{aligned} \tag{4.39}$$

As for the error bound $\mathcal{E}_Q^{s,b}(y)$, we also need to compute $||f(y)||_{L^\infty(D)}$ for $y \in \Gamma$, which is rather expensive. Alternatively, we can bound the second term $|(f(y), u(y) - u_Q(y))|$ in (B.4) by

$$\begin{aligned}|(f(y), u(y) - u_Q(y))| &= |(a(y)\nabla u(y), \nabla(u(y) - u_Q(y)))| \\ &\leq a_{max} C_2 ||u(y)||_X ||u(y) - u_Q(y)||_X \\ &\leq a_{max} C_2 (\mathcal{E}_Q^{u,b}(y) + \triangle_N^u(y) + ||u_{Q,N}||_X)\mathcal{E}_Q^{u,b}(y),\end{aligned} \tag{4.40}$$

where the first inequality follows from the definition of the constants a_{max} in (2.3) and C_2 in (A.12), while the second inequality holds because of the triangular inequality with the associated error bounds

$$||u(y)||_X \leq ||u(y) - u_Q(y)||_X + ||u_Q(y) - u_{Q,N}(y)||_X + ||u_{Q,N}(y)||_X. \tag{4.41}$$

20

In conclusion, a cheaper error bound for the output $\mathcal{E}_Q^{s,b}(y)$ reads

$$
\begin{aligned}
\mathcal{E}_Q^{s,b}(y) := {}& C_1 r_{Q_f+1}^f(x^{Q_f+1}, y^{Q_f+1})\left(\|u_{Q,N}(y)\|_X + \triangle_N^u(y)\right) \\
& + a_{max} C_2 \left(\|u_{Q,N}\|_X + \triangle_N^u(y) + \mathcal{E}_Q^{u,b}(y)\right)\mathcal{E}_Q^{u,b}(y).
\end{aligned}
\tag{4.42}
$$

4.3.4 On the evaluation of failure probability

In the evaluation of failure probability, the reduced basis method stays the same as presented in Algorithm 1, while the a posteriori error bound used in the hybrid reduced basis method in Algorithm 2 is modified as the global a posteriori error bound $\mathcal{E}_Q^{s,b} + \triangle_N^s$. In both methods, we prefer to construct a more accurate empirical interpolation for the non-affine random fields and a richer reduced basis space with small approximation error in order to improve the computational accuracy and efficiency, especially for $\mathcal{N}$ large entailing a costly solution of the full PDE. As for the goal-oriented reduced basis method, we adopt different computational strategies for different properties of the non-affine random fields.

When the random fields are rather regular (smooth manifold) with respect to the random vector y, the decay of the optimal approximation error or Kolmogorov width d_Q is very fast, so the empirical interpolation error also converges rapidly to zero thanks to proposition 4.2. In this case, the affine approximation error could be very small and dominated by the reduced basis approximation error. Therefore, goal-oriented adaptive reduced basis construction is still effectively governed by the a posteriori reduced basis approximation error bound. Whenever the distance between the approximate output and the critical value is smaller than the affine approximation error bound at sample $y \in \Gamma$, i.e. $|s_{Q,N}(y) - s_0| \leq \mathcal{E}_Q^{s,b}(y)$, which is extremely rare, we solve the full PDE to evaluate an accurate output.

On the other hand, if the non-affine random fields are far from smooth in the probability space, the affine approximation error bound $\mathcal{E}_Q^{s,b}(y)$ could be relatively large for small Q. In order to guarantee that the affine approximation error bound is dominated by the reduced basis approximation error bound, the number of the affine terms Q_a, Q_f might be very large, resulting in relatively more expensive online evaluation with $O((Q_f + NQ_a)^2)$ operations. In this circumstance, we choose to start from a crude approximation with small Q_a, Q_f, N for sake of computational efficiency and adaptively enrich the bases in the reduced basis space as well as refine the empirical interpolation with more affine terms governed by the error bounds $\triangle_N^s$ and $\mathcal{E}_Q^{s,b}$.

5 Numerical experiments

In this section, we carry out several numerical experiments to illustrate the computational difficulties encountered by conventional methods and demonstrate the accuracy and efficiency of our proposed methods for the evaluation of failure probability. Moreover, we apply our methods to more general PDE models of non-compliant, non-steady and non-affine types.

5.1 Benchmark models

5.1.1 One dimensional problems

First of all, we study the benchmark model of the elliptic problem (2.1) with different one dimensional random inputs. The physical domain is specified as a square $D = (0,1)^2$. We take a deterministic force term $f = 1$ for simplicity and consider the random diffusion coefficient a in different cases. The solution of the PDE model in physical domain is approximated by piecewise linear finite element functions. In probability domain Γ, we approximate the solution by stochastic collocation method introduced in section 2.2.3 and reduced basis method. For the latter, we use a uniform lower bound $\alpha_{LB} \leq \alpha(y), \forall y \in \Gamma$, for the sake of computational efficiency.

In the first test, we take a random field $a(x,y) = (1.1 + y\mathcal{X}_1(x))/10, x \in D, y \in \Gamma$ where y is a random variable uniformly distributed in $\Gamma = [-1, 1]$ and $\mathcal{X}_1$ is a characteristic function supported on a disk with radius 0.4 and center $(0.5, 0.5)$, i.e. $\mathcal{X}_1(x) = 1$ if $(x_1 - 0.5)^2 + (x_2 - 0.5)^2 \leq 0.4^2$, see
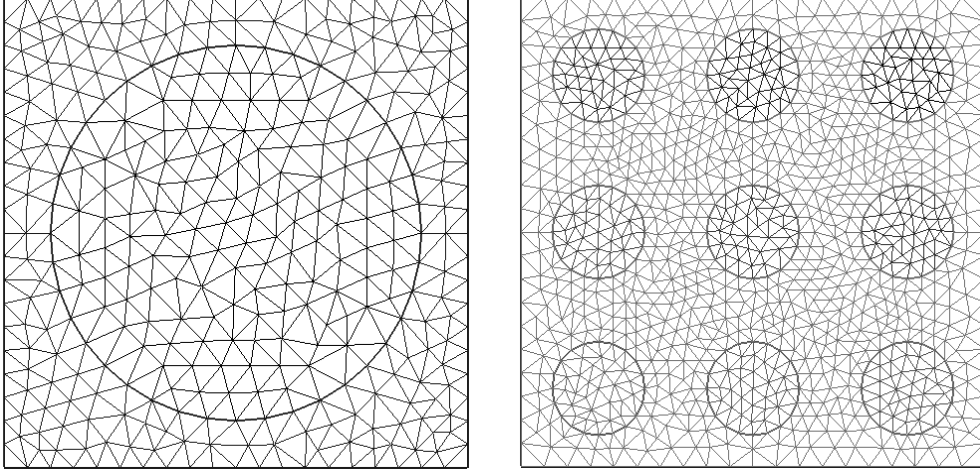
Figure 5.1: Finite element mesh for the physical domain D with 1 disk (left) and 9 disks (right)

the left of Figure 5.1. Note that the random field a is a first order polynomial of y, thus smooth in the probability domain Γ. In the second test, we take $a(x, y) = (1.1 + (1 - 2\mathcal{X}_{0.5}(y))\mathcal{X}_1(x))/10, x \in D, y \in \Gamma$, where the characteristic function $\mathcal{X}_{0.5}(y) = 1$ if $|y| \leq 0.5$. The random field a is now discontinuous in the probability domain Γ, in fact taking only two different values. The critical value of the output is taken as $s_0 = 0.2845$ in the first test and $s_0 = 0.2726$ in the second. For the approximation of the output s in probability domain, we first approximate the solution u by employing stochastic collocation method with hierarchical Clenshaw-Curtis rule [35], where the number of collocation nodes is $N = 2^n + 1, 1 \leq n \leq 5$, then evaluate the output $s_N = s(u_N)$ at the approximate solution u_N.
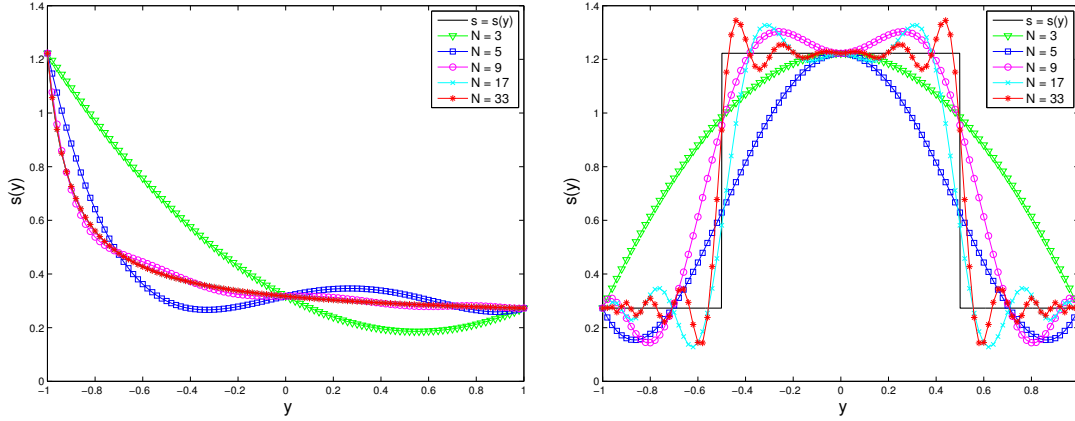
Figure 5.2: Stochastic collocation approximation of the output with different collocation nodes. Left, the random coefficient a is smooth; right, the random coefficient a is discontinuous in Γ.

Figure 5.2 displays the output $s(y), y \in \Gamma$ and the stochastic collocation approximation of the output for both the smooth and the discontinuous random fields. From the left of Figure 5.2, we can observe that the output approximated by stochastic collocation method converges to the accurate output when increasing the number of collocation nodes. The worst approximation error $\max_{y \in \Gamma} |s(y) - s_N(y)|$ computed in the sample set Ξ_{new} with $|\Xi_{new}| = 1000$ is shown in Table 5.1, which decreases to zero very fast and the failure probability $P(\omega \in \Omega : s(y(\omega)) < s_0)$ converges to the true value 0.20. As for the discontinuous test, we can see from the right of Figure 5.2 that the approximate output oscillates around and does not converge to the accurate output, because

of the Gibbs phenomenon (see also [16]). Due to the Gibbs phenomenon, the worst approximation error does not converge to zero but increases and the failure probability evaluated by the stochastic collocation method is far from the true value 0, as can be seen in Table 5.1 for Test 2. In order to compute an accurate failure probability, the threshold value in the hybrid approach must be so large that too many outputs (at samples in half of the probability domain in this example) have to be evaluated by fully solving the underlying PDE, which severely deteriorates the advantage of hybrid scheme. In the extreme case, the hybrid scheme may not gain any computational efficiency due to the fact that the outputs at most of the samples have to be evaluated by solving a full PDE.

Test \ Number of collocation nodes	$N = 3$	$N = 5$	$N = 9$	$N = 17$	$N = 33$
Test 1, $\max_{y \in \Gamma} \lvert s(y) - s_N(y) \rvert$	0.41	0.16	0.026	7.7e-4	6.3e-7
Test 1, $P(\omega \in \Omega : s(y(\omega)) < s_0)$	0.46	0.31	0.27	0.21	0.20
Test 2, $\max_{y \in \Gamma} \lvert s(y) - s_N(y) \rvert$	0.95	0.95	1.03	1.06	1.07
Test 2, $P(\omega \in \Omega : s(y(\omega)) < s_0)$	0.00	0.28	0.22	0.24	0.20

Table 5.1: Worst approximation error and failure probability of Test 1 (smooth) and Test 2 (discontinuous) evaluated by stochastic collocation method with different number of nodes.

In comparison, the worst approximation error for the output by reduced basis method (where we have set $\varepsilon_{tol} = 1.0 \times 10^{-14}$) decreases extremely fast, reaching 2.4×10^{-14} with only four bases in the first test of smooth random field, and it completely vanishes with only two bases in the second test of discontinuous random field. The failure probability evaluated by the reduced basis method is exact in both tests. This remarkable computational accuracy and efficiency can be attributed to the fact that the reduced basis method takes the solution (only two different solutions in the discontinuous case) as the approximation basis and solves a reduced PDE that inherits the same structure of the full PDE. Consequently, the reduced basis method overcomes the challenge of Gibbs phenomenon in the discontinuous case by avoiding the usage of dictionary basis.

5.1.2 Multidimensional problems

To further investigate the computational accuracy and efficiency of different methods for the evaluation of failure probability, we consider a multidimensional problem with many random inputs. The physical domain D and force term f are specified as in previous case. We suppose that there are nine disks in the domain (see the right of Figure 5.1) and define the background coefficient as $a_0(x, y) = 1, x \in D, y \in \Gamma$ and coefficients in the disks as $a_k(x, y) = 10^{y_k} \mathcal{X}_k(x), 1 \leq k \leq 9, x \in D, y \in \Gamma$, where $y_k, 1 \leq k \leq 9$ are independent and obeying uniform distribution in $\Gamma_k = [-2, 2]$, the characteristic functions are defined as $\mathcal{X}_k(x) = 1, (x_1 - x_1^k)^2 + (x_2 - x_2^k)^2 \leq 0.1^2$, with the centers at the points $((2i - 1)/6, (2j - 1)/6), 1 \leq i, j \leq 3$ where $3(i - 1) + j = k$. The random coefficient a is defined as $a = (a_0 + a_1 + \cdots + a_9)/10$.

In this numerical test, we employ the sparse grid stochastic collocation method introduced in section 2.2.3 to approximate the output s directly. 100 realizations of the random input $y \in \Gamma$ are sampled according to its probability distribution to specify the training set for the construction of the reduced basis space and another 100 realizations are sampled to test the two approximation methods. Figure 5.3 reports the comparison of the output error $\lvert s - s_N \rvert$ between stochastic collocation approximation and reduced basis approximation. On the left, the comparison is performed at one sample randomly chosen from the probability domain Γ, from which we can observe that the reduced basis approximation error decreases monotonically and much faster than the stochastic collocation approximation error, which starts to oscillate when the number of collocation nodes gets large due to over fitting problem. On the right, the comparison is carried out for the worst approximation error (the largest approximation error among 100 test samples randomly chosen in the probability domain), which shows that the reduced basis approximation is much more efficient than the stochastic collocation approximation in that only a small number (≤ 38) of the full PDEs need to be solved in order to gain the same worst approximation error compared to a significant large number (≥ 26017) of samples for the sparse grid collocation approach. The method becomes especially efficient when the solution lives in a low dimensional manifold while the random inputs
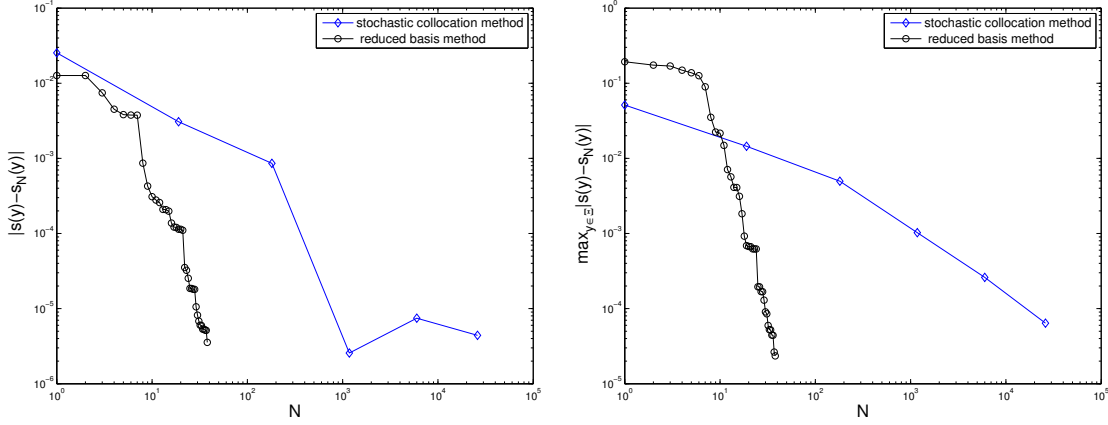
23

Figure 5.3: Comparison of output error between stochastic collocation approximation and reduced basis approximation. Left: error at one sample; right: worst approximation error.

are in high dimensions.

Figure 5.4 displays the effectivity of the employment of a posteriori error bound. On the left, we report the decay of the error bound $\triangle_N^s$ and the real output error $|s - s_N|$ with respect to the number of reduced basis functions at one sample randomly chosen from the probability domain. On the right, the effectivity defined as $\triangle_N^s/|s - s_N|$ at 100 test samples is shown. It proves that $\triangle_N^s \geq |s - s_N|$ for all the samples and the error bound $\triangle_N^s$ is not far from the real error $|s - s_N|$ at most of the samples, so that it is reasonable to use the a posteriori error bound for both certification of the approximation output and construction of the reduced basis space.
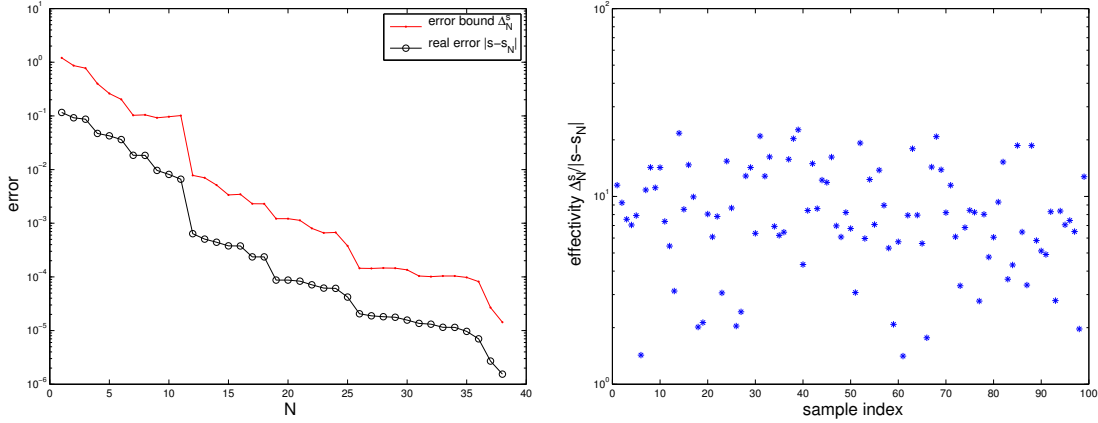
Figure 5.4: Left: comparison of error bound $\triangle_N^s$ and real error $|s - s_N|$ with repsect to the number of reduced basis functions N at one sample; right: effectivity $\triangle_N^s/|s - s_N|$ at 100 test samples.

For the evaluation of the failure probability, we test both the hybrid reduced basis method and the goal-oriented reduced basis method. From the same training set with 100 samples, we construct a fine reduced basis space with tolerance $\varepsilon_{tol} = 1 \times 10^{-4}$ for the former method, resulting in 38 bases, and a coarse reduced basis space with tolerance $\varepsilon_{tol} = 1 \times 10^{-2}$ for the latter method, leading to 18 bases. We compute the failure probability by hybrid algorithm 2 and goal-oriented adaptive Algorithm 3 by setting $M_0 = 1000$ initial samples, the scaling parameter $\beta = 4$ and a posterior error tolerance $\epsilon_{tol} = 1 \times 10^{-3}$. We remark that small value of the adaptive parameter β leads to a relatively small number of samples in each adaptation step, which is favorable for computational efficiency for the offline construction of the reduced basis space since there are less samples that need to be searched over. Large β potentially produces large difference of the a

posteriori error e_i^p in Algorithm 3, which drives I_{max} big and results in relatively more accurate failure probability. Here and in the following numerical experiments, we set $\beta = 4$ as a trade-off between computational efficiency and numerical accuracy. The comparison results are recorded in Table 5.2, from which we can see that the reduced basis space for the hybrid method is fine enough and we only need to solve 329 full PDEs in total in order to evaluate the outputs at 341000 samples. By the goal-oriented adaptive approach, the total number of full PDEs that should be solved is 132. Nevertheless, only 36 PDEs need a full solving thanks to the adaptation of the reduced basis space at each iteration, which achieves further computational efficiency. Moreover, owing to an effective and cheap a posteriori error bound, both the hybrid approach and the goal-oriented adaptive approach result in the same failure probability (0.027 for a critical value $s_0 = 0.25$) as being solved directly by Monte Carlo method. In summary, both the hybrid and the goal-oriented adaptive reduced basis methods have been successfully applied to efficiently and accurately compute the failure probability, with the goal-oriented adaptive approach gaining remarkable computational efficiency thus more suitable to solve complex PDEs with time-consuming solver.

Number of Monte Carlo samples	$1M_0$	$4M_0$	$16M_0$	$64M_0$	$256M_0$	$341M_0$
Hybrid RBM, # $(|s - s_N| < \triangle_N^s)$	0	3	22	59	245	329
Adaptive RBM, # $(|s - s_N| < \triangle_N^s)$	41	41	20	8	22	132
Adaptive RBM, # adapted bases	8	9	6	5	8	36
Failure probability $P_0^m = P_0^h = P_0^g$	0.043	0.033	0.030	0.027	0.027	0.027

Table 5.2: Comparison between hybrid RBM and goal-oriented adaptive RBM in terms of the number of samples for which the full PDE have to be solved; $M_0 = 1000$.

5.2 Non-compliant problems

We take $D = (0,1)^2$ and suppose that the covariance fields of the random inputs are available and both the diffusion coefficient a and the force term f are obtained from truncation of the Karhunen-Loève expansion of covariance fields [53], expressed as

$$a(x, y(\omega)) = \mathbb{E}[a] + \sum_{q=1}^{Q_a} \sqrt{\lambda_q^a} a_q(x) y_q(\omega) \text{ and } f(x, y(\omega)) = \mathbb{E}[f] + \sum_{q=1}^{Q_f} \sqrt{\lambda_q^f} f_q(x) y_q^f(\omega), \qquad (5.1)$$

where $(\lambda_q^a, a_q)_{q=1}^{Q_a}$ and $(\lambda_q^f, f_q)_{q=1}^{Q_f}$ are the eigenvalues and orthonormal eigenfunctions associated to their corresponding covariance fields, $y_q^a, 1 \leq q \leq Q_a$ and $y_q^f, 1 \leq q \leq Q_f$ are mutually uncorrelated with mean zero and unit variance. For the $i-$th coordinate, $i = 1, \ldots, d$, the general formula of a Gaussian random field $g(x_i, y)$ is written as [35]

$$g(x_i, y) = \mathbb{E}[g] + \left(\frac{\sqrt{\pi}L}{2}\right)^{1/2} y_1^g(\omega) + \sum_{k=1}^{K} \sqrt{\lambda_n} \left(\sin(k\pi x_i) y_{2k}^g(\omega) + \cos(k\pi x_i) y_{2k+1}^g(\omega)\right). \qquad (5.2)$$

where the random variables $y_k^g, 1 \leq k \leq 2K + 1$ are assumed to be uniformly distributed in $[-\sqrt{3}, \sqrt{3}]$. For simplicity, we assume that the covariance fields for a and f are Gaussian fields depending on x_1 coordinate and x_2 coordinate, respectively, with the same correlation length $L = 1/4$ and eigenvalues $\lambda_1 = 0.3798, \lambda_2 = 0.2391, \lambda_3 = 0.1106, \lambda_4 = 0.0376, \lambda_5 = 0.0094, \lambda_6 = 0.0017$, etc. We take $Q_a = Q_f = 13$ with $K = 6$ in (5.2) leading to a 26 dimensional problem, which accounts for around 99% uncertainties of the random field. The expectation of the random force f given by (5.2) is taken as $\mathbb{E}[f] = 6$; the expectation of a random field $\tilde{a}$ given by (5.2) is specified as $\mathbb{E}[\tilde{a}] = 5$ and we take $a = \tilde{a}/10$. The output $s(y) = s(u(y)) = \int_D 10u(x, y)dx$ is different from the force term.

We adopt the primal-dual computational strategy for non-compliant problems presented in section 4.1. We set the tolerance $\varepsilon_{tol} = 1 \times 10^{-4}$ for $||R^{pr}||_{X'}^2/\alpha_{LB}$ and $||R^{du}||_{X'}^2/\alpha_{LB}$ (see the
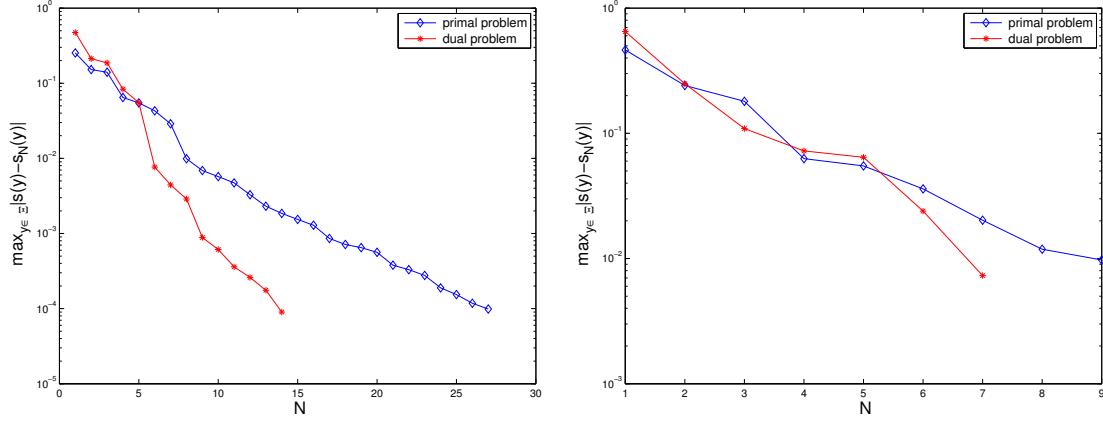
Figure 5.5: Worst primal-dual reduced basis approximation error of hybrid type with $\varepsilon_{tol} = 1 \times 10^{-4}$ (left) and goal-oriented adaptive type with $\varepsilon_{tol} = 1 \times 10^{-2}$ (right) at 100 test samples.

definition of residual in (4.6)) in the hybrid reduced basis method and $\varepsilon_{tol} = 1 \times 10^{-2}$ in the goal-oriented adaptive reduced basis method. The constructed hybrid reduced basis space for the primal problem contains 27 bases and 14 bases for the dual problem, while for the construction of the goal-oriented adaptive reduced basis method, there are 9 and 7 bases respectively. We test the reduced basis approximation for both the primal and the dual problems with 100 test samples and present the worst approximation errors in Figure 5.5, which illustrates the exponentially fast convergence of the reduced basis approximation in high dimensional random inputs. Figure 5.6 depicts the dependence of the worst approximation error for the output $\max_{y \in \Xi_{test}} |s(y) - s_N(y)|$ (Ξ_{test} denotes the test sample set with 100 samples) with respect to the number of bases in the primal and dual reduced basis space (left) as well as the effectivity of the a posterior error bound defined as $\triangle_N^s(y)/|s(y) - s_N(y)|$ (right), from which we can observe that simultaneous increase of the bases in both primal and dual reduced basis spaces not only leads to faster convergence of the output approximation error but also improves the sharpness of the a posteriori error bound, thus enhances the computational efficiency for the evaluation of the failure probability.
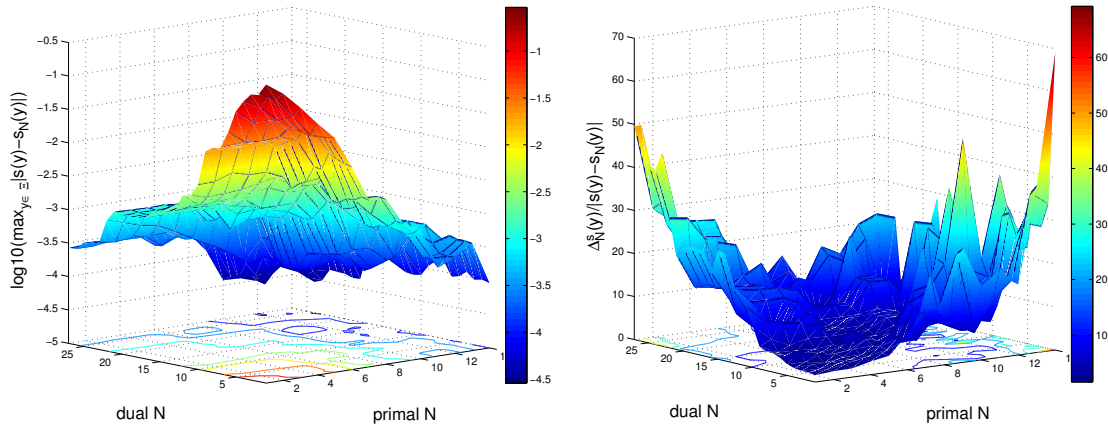

Figure 5.6: Worst primal-dual reduced basis approximation error of hybrid type with $\varepsilon_{tol} = 1 \times 10^{-4}$ (left) and goal-oriented adaptive type with $\varepsilon_{tol} = 1 \times 10^{-2}$ (right) at 100 test samples.

The error tolerance for the failure probability is set to $\epsilon_{tol} = 1 \times 10^{-4}$ with a critical value $s_0 = 4$. We test both the hybrid and the goal-oriented adaptive approaches, with the results recorded in Table 5.3. Due to the fact that the solution lies in a very low dimensional stochastic manifold, the

fine hybrid reduced basis approximate output is very close to the true value and there are only 52 out of 1365000 samples that cannot be determined; as for the goal-oriented adaptive approach, 48 samples can be not determined and only 21 PDEs are fully solved for adaptation of the primal and dual reduced basis spaces. From this experiment, we can see that we don't gain much more computational efficiency by the goal-oriented adaptive method than by the hybrid method, so that it's sufficient to use the hybrid reduced basis method to compute failure probability for problems with very smooth solution in the probability space.

Number of Monte Carlo samples	$1M_0$	$4M_0$	$16M_0$	$64M_0$	$256M_0$	$1024M_0$	$1365M_0$
Hybrid RBM, # $(|s - s_N| < \triangle_N^s)$	1	0	0	1	11	39	52
Adaptive RBM, # $(|s - s_N| < \triangle_N^s)$	3	4	7	5	15	14	48
Adaptive RBM, # adapted bases	2	1	3	4	6	5	21
Failure probability $P_0^m = P_0^h = P_0^g$	0.361	0.372	0.3823	0.3864	0.3832	0.3831	0.3831

Table 5.3: Comparison between hybrid RBM and goal-oriented adaptive RBM in terms of the number of samples for which the full PDE have to be solved; $M_0 = 1000$.

5.3 Non-steady problems

We consider a heat transfer problem in a thermal fin with the geometry displayed in Figure 5.7, where the thermal conductivity in the main body and the four extended surfaces depends on five independent random variables obeying uniform distribution in $[-2, 2]$, i.e.

$$a_0(x, y) = 1 + 10^{y_0}\mathcal{X}_0(x), \text{ and } a_k(x, y) = 10^{y_k}\mathcal{X}_k(x), 1 \le k \le 4,$$

where the characteristic functions $\mathcal{X}_k, 0 \le k \le 4$ are supported in the sub domains $D_k, 0 \le k \le 4$. Moreover, we consider the Biot number on the Robin boundaries as a random field as

$$b(x, y) = 10^{y_5}\mathcal{X}_{\partial D_r}(x),$$

where the characteristic function $\mathcal{X}_{\partial D_r}(x)$ is supported on the Robin boundaries. The time dependent heat transfer problem is formulated in the strong form as

$$\frac{\partial u(t, x, y)}{\partial t} - \sum_{k=0}^{4} \nabla(a_k(x, y)\nabla u(t, x, y)) = 0, \quad (t, x) \in [0, T] \times D, \text{ a.s. } y \in \Gamma, \qquad (5.3)$$

where $\Gamma = [-2, 2]^6$; we take $T = 5$ and impose homogeneous initial condition $u(0, x, y) = 0$ everywhere; we also prescribe heat flux $f(x) = 1, x \in \partial D_n^1$ at the bottom edge, homogeneous Neuman boundary condition on the boundary ∂D_n^2 and the following Robin boundary condition on the boundary of the extended surfaces ∂D_r

$$\sum_{k=0}^{4} a_k(x, y)\nabla u(t, x, y) \cdot \mathbf{n} + b(x, y)u(t, x, y) = 0, \quad (t, x) \in [0, T] \times \partial D_r, \text{ a.s. } y \in \Gamma,$$

By the first order backward Euler scheme for time discretization with time step $\Delta t = 0.05$, we can write the semi-weak formulation of the problem (5.3) as: find $u^i(y) \in X, 1 \le i \le 100$ such that the following equation holds almost surely $y \in \Gamma$

$$M(u^i(y), v; y) + \Delta t\sum_{k=0}^{4} A_k(u^i(y), v; y) + \Delta tB(u^i(y), v; y) = \Delta tF(v; y) + M(u^{i-1}(y), v; y), v \in X$$

$$(5.4)$$

where $B(u^i(y), v; y) = \int_{\partial D_r} b(x, y)u^i(x, y)v(x)dx$ and $F(v; y) = \int_{\partial D_n^1} f(x)v(x)dx$.
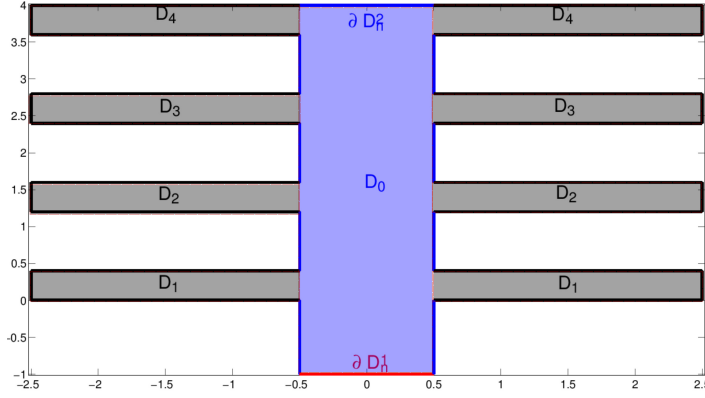
27

Figure 5.7: Geometry of a thermal fin, with domain D_0 (blue) defined as the main body, $D_k, 1 \leq k \leq K$ (black) as the extended surfaces, ∂D_n^1 (red) where imposing heat flux, ∂D_n^2 (blue) for homogeneous Neuman boundary conditions and the left boundary ∂D_r as Robin boundary.

We define the compliant output as the integrated temperature over the flux boundary at the upper time $T = 5$, i.e. $s(y) = s(T; y) = F(u(T; y); y)$, and consider a critical value $s_0 = 2.3$ with failure probability (ineffective heat transfer) defined as $P_f(\omega \in \Omega : s(y(\omega)) > s_0)$. Figure 5.8 displays temperature distribution at three different samples at the end of the simulation, being the first one very effective for heat transfer and the last one ineffective.
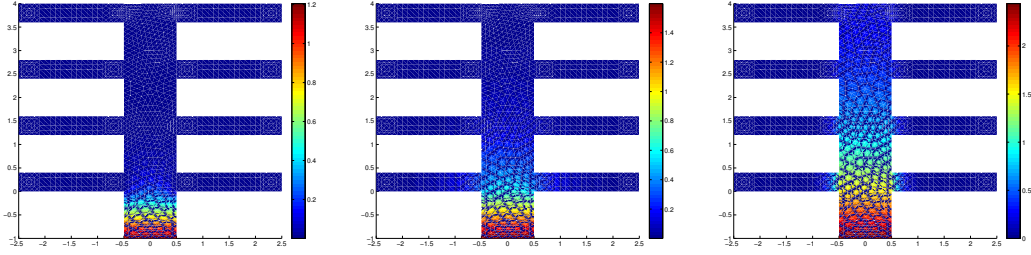
Figure 5.8: Temperature distribution at $T = 5$ for three different samples: left, $y_k = 2$, effective heat transfer; middle, reference $y_k = 0$; right, $y_k = -2, 0 \leq k \leq 5$, ineffective heat transfer.

Number of Monte Carlo samples	$1M_0$	$4M_0$	$16M_0$	$64M_0$	$256M_0$	$341M_0$
Hybrid RBM, # ($|s - s_N| < \triangle_N^s$)	0	600	1500	3800	12400	18300
Adaptive RBM, # ($|s - s_N| < \triangle_N^s$)	700	1200	500	2300	1400	6100
Adaptive RBM, # PDE solves	400	400	200	700	300	2000
Adaptive RBM, # adapted bases	13	39	10	37	28	127
Failure probability $P_0^m = P_0^h = P_0^g$	0.0280	0.0315	0.0288	0.0304	0.0308	0.0308

Table 5.4: Comparison between hybrid RBM and goal-oriented adaptive RBM in terms of the number of samples for which the full PDE have to be solved; $M_0 = 1000$.

We build the reduced basis space for hybrid method with tolerance $\varepsilon_{tol} = 1 \times 10^{-4}$, resulting in 93 bases as shown in the left of Figure 5.9; as for goal-oriented adaptive method, we set the tolerance $\varepsilon_{tol} = 1 \times 10^{-2}$, leading to 42 initial bases. The effectivity for a posteriori error bound at 100 test samples is displayed in the right of Figure 5.9, which are sharp and distributed close to a constant smaller than 10. The results for the evaluation of failure probability with a tolerance $\epsilon_{tol} = 1 \times 10^{-3}$ are shown in Table 5.4, from which we can see that the goal-oriented adaptive
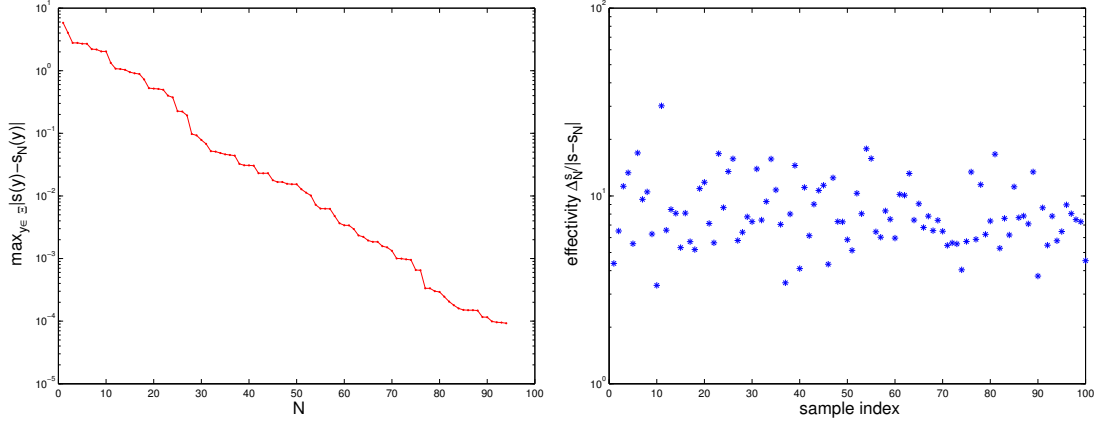
Figure 5.9: Left: decay of worst approximation error $\max_{y\in\Xi_{test}}|s(y)-s_N(y)|$ with respect to the number of reduced basis functions N; right: error bound effectivity $\triangle_N^s/|s-s_N|$ at 100 samples.

approach is much more efficient than the hybrid approach, solving only 2000 full PDEs (5.4) instead of 18300 in the latter approach. We remark that the number of full PDE solves (2000 in total) is different from the number of adapted bases (127 in total) in goal-oriented adaptive reduced basis method for non-steady problems.

5.4 Non-affine problems

Instead of the affine expansion (5.1) of the random fields a and f, we consider the Karhunen-Loève expansion for the logarithmic function of the random fields a and f, written as follows:

$$\log\left(a(x,y(\omega))-\mathbb{E}[a]\right)=C_a\sum_{q=1}^{P_a}\sqrt{\lambda_q^a}a_q(x)y_q(\omega),$$

$$\log\left(f(x,y(\omega))-\mathbb{E}[f]\right)=C_f\sum_{q=1}^{P_f}\sqrt{\lambda_q^f}f_q(x)y_q^f(\omega),$$

which are widely used in practical engineering models [35] in that the random fields are guaranteed to be positive, so that the random variables in the Gaussian random field expansion (5.2) are allowed to be standard Gaussian random variables with zero mean and unit variance. We take a correlation length $L=1/16$ smaller than in section 5.2 for both the diffusion random coefficient $a(x_1,y)$ depending only in x_1 and the random force $f(x_2,y)$ depending only in x_2 in the formula (5.2). This leads to $P_a=P_f=51$ terms to cover 99% of the total randomness, thus yielding a high dimensional stochastic problem with $P_a+P_f=102$ independent standard Gaussian random variables in total. The physical domain is set as $D=(0,1)^2$.

We perform an empirical interpolation procedure to affinely decompose the non-affine random fields a (with $C_a=50$ and $\mathbb{E}[a]=0.1$) and f (with $C_f=20$ and $\mathbb{E}[f]=0.1$) with error tolerance $\varepsilon_{tol}=1\times10^{-8}$ in Algorithm 5. The decay of the error bound $r_{Q+1}(x^{Q+1},y^{Q+1})$ and the worst approximation error $\max_{y\in\Xi_{test}}||g(y)-g_Q(y)||_{L^\infty(D)}$ computed in a test set Ξ_{test} with 100 samples are displayed in Figure 5.10, from which we can see that the empirical interpolation reaches very small error (1×10^{-8}) by only a few affine terms, $Q_a=33$ for a_{Q_a} and $Q_f=17$ for f_{Q_f} in (4.31), which are smaller than 51. By setting $\Theta_q^a,1\leq q\leq33$ and $\Theta_q^f,1\leq q\leq17$ as new random variables in the affine decomposition formula (4.31), we can view the empirical interpolation as an efficient dimension reduction method in order to alleviate the curse-of-dimensionality, especially when the manifold of stochastic solution is in low dimensional probability space. Moreover, the error bound $r_{Q+1}(x^{Q+1},y^{Q+1})$ is accurate and very sharp (close to the worst approximation error) as can be
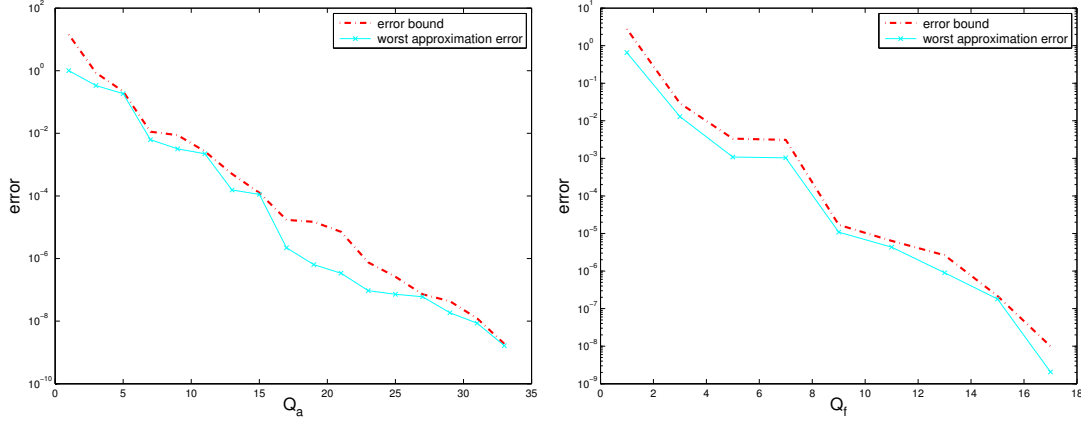
Figure 5.10: Decay of the error bound $r_{Q+1}(x^{Q+1}, y^{Q+1})$ and the worst approximation error $\max_{y \in \Xi_{test}} \|g(y) - g_Q(y)\|_{L^\infty(D)}$ for a (left) and f (right) by empirical interpolation method.

observed from Figure 5.10, so that the cheap a posteriori error bounds constructed in (4.39) and (4.42) are also accurate and sharp.
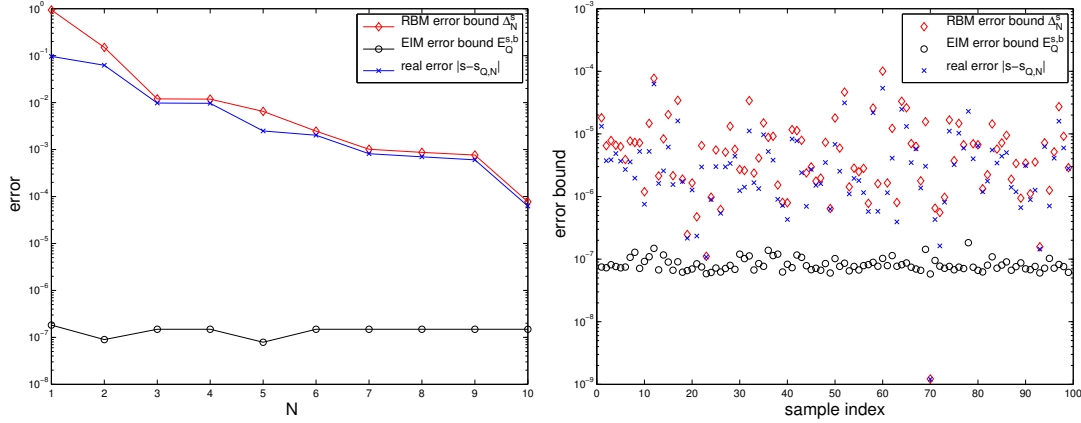

Figure 5.11: Worst approximation error $|s - s_{Q,N}|$, reduced basis error bound $\triangle_N^s$ and empirical interpolation error bound $\mathcal{E}_Q^{s,b}$ for N reduced basis functions (left), and at 100 test samples (right).

To evaluate the a posteriori error bound $\mathcal{E}_Q^{s,b}$ in (4.42) from the contribution of affine decomposition, we first compute $C_1 = 1$, $C_2 = 1$ from (A.18) and bound a almost surely by the estimate $a_{max} = 10$; the bound for the empirical interpolation error are taken from the construction of the affine decomposition as $r_{Q_a+1}^a(x^{Q_a+1}, y^{Q_a+1}) = 1.9 \times 10^{-9}$ and $r_{Q_f+1}^f(x^{Q_f+1}, y^{Q_f+1}) = 9.9 \times 10^{-9}$. We construct the reduced basis space with error tolerance $\varepsilon_{tol} = 1 \times 10^{-4}$, leading to 10 bases as shown on the left of Figure 5.11, where the reduced basis error bound $\triangle_N^s(y)$ as well as the empirical interpolation error bound $\mathcal{E}_Q^{s,b}(y)$ are also shown at the sample y that leads to the worst approximation real error $y = \arg\max_{y \in \Xi_{test}} |s(y) - s_{Q,N}(y)|$. It can be observed that the empirical interpolation error bound $\mathcal{E}_Q^{s,b}$ is much smaller than the reduced basis error bound $\triangle_N^s$, so that we can enrich the reduced basis space in order to obtain better approximation of the output with certified small error from affine decomposition. On the right of Figure 5.11, the different error bounds computed with 10 bases in the reduced basis space as well as the real output error are displayed at 100 test samples, which confirms the observation of the left figure for most of the samples (with one exception where the reduced basis approximation of the output is extremely close to the real output). Moreover, we can see that the reduced basis error bound is accurate and

sharp, being very close to the real error at most of the samples. In order to evaluate the failure probability with critical value $s_0 = 0.3$ and tolerance $\epsilon_{tol} = 1 \times 10^{-3}$, we set the reduced basis construction tolerance $\varepsilon_{tol} = 1 \times 10^{-4}$ for hybrid approach, resulting in 10 bases and $\varepsilon_{tol} = 1 \times 10^{-2}$ for goal-oriented adaptive approach with 4 bases. The results are displayed in Table 5.5, which shows that the reduced basis space is in very low dimensions (only 10 dimensions for the hybrid approach and $4 + 7 = 11$ dimensions for the goal-oriented adaptive approach) due to the fact that the stochastic solution and output live in a very low dimensional manifold, even though the random inputs are in high dimensions.

Number of Monte Carlo samples	$1M_0$	$4M_0$	$16M_0$	$64M_0$	$256M_0$	$341M_0$
Hybrid RBM, # $(|s - s_N| < \triangle_N^s)$	0	1	1	7	33	42
Adaptive RBM, # $(|s - s_N| < \triangle_N^s)$	13	2	5	1	14	35
Adaptive RBM, # adapted bases	2	1	1	1	2	7
Failure probability $P_0^m = P_0^h = P_0^g$	0.064	0.059	0.062	0.065	0.064	0.064

Table 5.5: Comparison between hybrid RBM and goal-oriented adaptive RBM in terms of the number of samples for which the full PDE has to be solved; $M_0 = 1000$.

6   Concluding remarks

In this paper we developed hybrid and goal-oriented adaptive computational strategies based on reduced basis method to efficiently and accurately compute the failure probability of partial differential equations with random inputs. In particular, we designed an efficient sampling scheme by the goal-oriented greedy algorithm to construct an accurate reduced basis model to approximate the stochastic output, especially for high dimensional problems with many random inputs. In order to compute the failure probability of low regularity system with respect to the random inputs, we developed a hybrid approach with goal-oriented adaptation governed by cheap and sharp a posteriori error bound for both the construction of reduced basis space and the approximation of the output with certification. We extended the proposed methods to more general PDE models of non-compliant, non-steady and non-affine types, using appropriate techniques. In the numerical experiments, we studied different PDEs with uncertainties from physical parameters, external loadings, boundary conditions as random inputs obeying uniform distribution and normal distribution. However, the numerical experiments are based on simple academic examples with specific design for testing the computational properties of our proposed methods. Further research will be devoted to the development and application of our methods in practical engineering problems with more general PDE models and random inputs. It is worth to mention that Monte Carlo error plays a significant role in accurate evaluation of rare failure probability of extreme events. We will address this issue by efficiently combining model reduction with importance sampling techniques in the coming work [13], where the proposed reduced basis method is used to reduce the cost in solving the underlying PDE model and adaptive cross-entropy method is employed to reduce the number of Monte Carlo samples. We also remark that we didn't take temporal and spatial discretization errors into account, which might be important, e.g. in highly nonlinear or advection-dominated problems. To carry out a global error analysis and design suitable global error bounds are helpful for more rigorous evaluation of failure probability.

A Proof of Lemma 4.3

Proof The total approximation error can be bounded by the sum of two terms

$$||u(y) - u_{Q,N}(y)||_X \leq ||u(y) - u_Q(y)||_X + ||u_Q(y) - u_{Q,N}(y)||_X, \tag{A.1}$$

the former due to the affine approximation error of the random fields a and f, the latter arising from the reduced basis approximation error. Using (3.11), we have

$$||u_Q(y) - u_{Q,N}(y)||_X \leq \triangle_N^u. \tag{A.2}$$

Thus, we only need to control the first part with an error bound denoted as

$$||u(y) - u_Q(y)||_X \leq \mathcal{E}_Q^u(y). \tag{A.3}$$

To bound the first term, we consider the weak formulation of the problem (2.1) with the original random fields a and f as well as the approximate a_{Q_a} and f_{Q_a},

$$(a\nabla u, \nabla v) = (f, v) \quad \forall v \in H_0^1(D) \tag{A.4}$$

and

$$(a_{Q_a}\nabla u_Q, \nabla v) = (f_{Q_f}, v) \quad \forall v \in H_0^1(D) \tag{A.5}$$

respectively. Subtracting (A.5) from (A.4), we have

$$(a\nabla u - a_{Q_a}\nabla u_Q, \nabla v) = (f - f_{Q_f}, v) \quad \forall v \in H_0^1(D), \tag{A.6}$$

which can be transformed by adding and subtracting $a\nabla u_Q$ as

$$(a\nabla(u - u_Q), \nabla v) = (f - f_{Q_f}, v) + ((a_{Q_a} - a)\nabla u_Q, \nabla v) \quad \forall v \in H_0^1(D). \tag{A.7}$$

Taking $v = u - u_Q$ in (A.7) and applying the coercive property of the left hand side, we have

$$l.h.s. \geq \alpha(y)||u(y) - u_Q(y)||_X^2 \geq \alpha_{LB}(y)||u(y) - u_Q(y)||_X^2. \tag{A.8}$$

As for the right hand side of (A.7), we have the following bound by Cauchy-Schwarz inequality,

$$\begin{aligned} r.h.s \leq &||f(y) - f_{Q_f}(y)||_{L^\infty(D)}||u(y) - u_Q(y)||_{L^1(D)} \\ &+ ||a(y) - a_{Q_a}(y)||_{L^\infty(D)}||\nabla u_Q(y)||_{L^2(D)}||\nabla(u(y) - u_Q(y))||_{L^2(D)}. \end{aligned} \tag{A.9}$$

By Poincaré inequality [1], we have that

$$||u(y) - u_Q(y)||_{L^1(D)} \leq C_P||\nabla(u(y) - u_Q(y))||_{L^1(D)} \tag{A.10}$$

where $C_P \leq d_D/2$ with d_D standing for the diameter of the domain D. Moreover, we have again by Cauchy-Schwarz inequality the following relation

$$||\nabla(u(y) - u_Q(y))||_{L^1(D)} \leq C_D||\nabla(u(y) - u_Q(y))||_{L^2(D)}, \tag{A.11}$$

where $C_D = \sqrt{|D|}$ with $|D|$ representing the Lebesgue measure of the domain D. By the definition of the norm $||v||_X = \sqrt{(a(\bar{y})\nabla v, \nabla v)}$ at a reference value $\bar{y} \in \Gamma$, we have

$$||\nabla v||_{L^2(D)} \leq C_X||v||_X \quad \forall v \in H_0^1(D), \tag{A.12}$$

where $C_X \leq \sqrt{||1/a(\bar{y})||_{L^\infty(D)}}$. Using the inequalities (A.10), (A.11) and (A.12), we have the following bound for the right hand side (A.9)

$$
\begin{aligned}
r.h.s \leq &\ C_D C_P C_X ||f(y) - f_{Q_f}(y)||_{L^\infty(D)} ||u(y) - u_Q(y)||_X \\
&+ C_X^2 ||a(y) - a_{Q_a}(y)||_{L^\infty(D)} ||u_Q(y)||_X ||u(y) - u_Q(y)||_X.
\end{aligned}
\tag{A.13}
$$

Furthermore, by setting $v = u_Q$ in the weak formulation (A.5), we obtain

$$
||u_Q(y)||_X \leq \frac{C_D C_P C_X}{\alpha_{LB}(y)} ||f_{Q_f}(y)||_{L^\infty(D)},
\tag{A.14}
$$

for which we have used the following coercive property with lower bound $\alpha_{LB}(y) \leq \alpha_{Q_a}(y)$

$$
(a_{Q_a} \nabla u_Q, \nabla u_Q) \geq \alpha_{Q_a}(y) ||u_Q(y)||_X^2 \geq \alpha_{LB}(y) ||u_Q(y)||_X^2
\tag{A.15}
$$

as well as the following bound by the inequalities (A.10), (A.11) and (A.12)

$$
(f_{Q_f}, u_Q) \leq ||f_{Q_f}(y)||_{L^\infty(D)} ||u_Q(y)||_{L^1(D)} \leq C_D C_P C_X ||f_{Q_f}(y)||_{L^\infty(D)} ||u_Q(y)||_X.
\tag{A.16}
$$

A combination of (A.13) and (A.14) leads to the following bound for the right hand side of (A.7)

$$
\begin{aligned}
r.h.s \leq &\ C_D C_P C_X ||f(y) - f_{Q_f}(y)||_{L^\infty(D)} ||u(y) - u_Q(y)||_X \\
&+ \frac{C_D C_P C_X^3}{\alpha_{LB}(y)} ||a(y) - a_{Q_a}(y)||_{L^\infty(D)} ||f_{Q_f}(y)||_{L^\infty(D)} ||u(y) - u_Q(y)||_X.
\end{aligned}
\tag{A.17}
$$

By comparing the left hand side (A.8) and the right hand side (A.17), we obtain the error bound (4.33) depending only on the data a, f and their empirical interpolation errors, where C_1 and C_2 are defined as

$$
C_1 := C_D C_P C_X \leq \sqrt{|D|} \frac{d_D}{2} \sqrt{\left|\left|\frac{1}{a(\bar{y})}\right|\right|_{L^\infty(D)}} \quad \text{and} \quad C_2 := C_X^2 \leq \left|\left|\frac{1}{a(\bar{y})}\right|\right|_{L^\infty(D)}.
\tag{A.18}
$$

$\square$

B   Proof of Lemma 4.4

Proof Similar to the proof of Lemma 4.3, we split the output approximation error into

$$
|s(y) - s_{Q,N}(y)| \leq |s(y) - s_Q(y)| + |s_Q(y) - s_{Q,N}(y)|,
\tag{B.1}
$$

where the first part corresponds to the affine approximation error of the random fields a and f and the second part arises from the reduced basis approximation error bounded by

$$
|s_Q(y) - s_{Q,N}(y)| \leq \triangle_N^s(y),
\tag{B.2}
$$

which can be evaluated from (3.12). As for the first part, we seek a bound denoted as

$$
|s(y) - s_Q(y)| \leq \mathcal{E}_Q^s(y).
\tag{B.3}
$$

By definition of the output $s = (f, u)$ and the approximate output $s_Q = (f_{Q_f}, u_Q)$, we have

$$
\begin{aligned}
|s(y) - s_Q(y)| &= |(f(y), u(y)) + (f_{Q_f}(y), u_Q(y))| \\
&\leq |(f(y) - f_{Q_f}(y), u_Q(y))| + |(f(y), u(y) - u_Q(y))| \\
&\leq ||f(y) - f_{Q_f}(y)||_{L^\infty(D)}||u_Q(y)||_{L^1(D)} + ||f(y)||_{L^\infty(D)}||u(y) - u_Q(y)||_{L^1(D)} \\
&\leq C_1||f(y) - f_{Q_f}(y)||_{L^\infty(D)}||u_Q(y)||_X + C_1||f(y)||_{L^\infty(D)}||u(y) - u_Q(y)||_X \\
&\leq \frac{C_1^2}{\alpha_{LB}(y)}||f(y) - f_{Q_f}(y)||_{L^\infty(D)}||f_{Q_f}(y)||_{L^\infty(D)} + C_1||f(y)||_{L^\infty(D)}\mathcal{E}_{a,f}^u(y),
\end{aligned}
\tag{B.4}
$$

where the first inequality is due to the triangular inequality, the second one to the Cauchy-Schwarz inequality, the third one follows from combining (A.10), (A.11) and (A.12), and the fourth inequality follows from using (A.14) and the error bound (A.3). □

References

[1] G. Acosta and R.G. Durán. An optimal Poincaré inequality in L1 for convex domains. *Proceedings of the American Mathematical Society*, pages 195–202, 2004.

[2] I. Babuška, F. Nobile, and R. Tempone. A stochastic collocation method for elliptic partial differential equations with random input data. *SIAM Journal on Numerical Analysis*, 45(3):1005–1034, 2007.

[3] I. Babuška, R. Tempone, and G.E. Zouraris. Galerkin finite element approximations of stochastic elliptic partial differential equations. *SIAM Journal on Numerical Analysis*, 42(2):800–825, 2005.

[4] M. Barrault, Y. Maday, N.C. Nguyen, and A.T. Patera. An empirical interpolation method: application to efficient reduced-basis discretization of partial differential equations. *Comptes Rendus Mathematique, Analyse Numérique*, 339(9):667–672, 2004.

[5] J. Beck, F. Nobile, L. Tamellini, and R. Tempone. Stochastic spectral Galerkin and collocation methods for PDEs with random coefficients: A numerical comparison. *Spectral and High Order Methods for Partial Differential Equations. Springer*, 76:43–62, 2011.

[6] P. Binev, A. Cohen, W. Dahmen, R. DeVore, G. Petrova, and P. Wojtaszczyk. Convergence rates for greedy algorithms in reduced basis methods. *SIAM Journal of Mathematical Analysis*, 43(3):1457–1472, 2011.

[7] S. Boyaval, C. LeBris, Y. Maday, N.C. Nguyen, and A.T. Patera. A reduced basis approach for variational problems with stochastic parameters: Application to heat conduction with variable Robin coefficient. *Computer Methods in Applied Mechanics and Engineering*, 198(41-44):3187–3206, 2009.

[8] C.G. Bucher and U. Bourgund. A fast and efficient response surface approach for structural reliability problems. *Structural Safety*, 7(1):57–66, 1990.

[9] O. Cappé, R. Douc, A. Guillin, J.M. Marin, and C.P. Robert. Adaptive importance sampling in general mixture classes. *Statistics and Computing*, 18(4):447–459, 2008.

[10] P. Chen, A. Quarteroni, and G. Rozza. Comparison between reduced basis and stochastic collocation methods for elliptic problems. *Journal of Scientific Computing, DOI 10.1007/s10915-013-9764-2*, 2013.

[11] P. Chen, A. Quarteroni, and G. Rozza. A weighted empirical interpolation method: A priori convergence analysis and applications. *EPFL, MATHICSE Report 05, submitted*, 2013.

[12] P. Chen, A. Quarteroni, and G. Rozza. A weighted reduced basis method for elliptic partial differential equations with random input data. *EPFL, MATHICSE Report 04, submitted*, 2013.

[13] P. Chen, and A. Quarteroni Accruate and efficient evaluation of rare failure probability for partial differential equations with random input data. *In preparation*, 2013.

[14] Y. Chen, J.S. Hesthaven, Y. Maday, and J. Rodríguez. Certified reduced basis methods and output bounds for the harmonic Maxwell's equations. *SIAM Journal on Scientific Computing*, 32(2):970–996, 2010.

[15] A. Cohen, R. Devore, and C. Schwab. Analytic regularity and polynomial approximation of parametric and stochastic elliptic PDE's. *Analysis and Applications*, 9(01):11–47, 2011.

[16] R.A. DeVore and G.G. Lorentz. *Constructive Approximation*. Springer, 1993.

[17] O.G. Ernst, C.E. Powell, D.J. Silvester, and E. Ullmann. Efficient solvers for a linear stochastic galerkin mixed formulation of diffusion problems with random data. *SIAM Journal of Scientific Computing*, 31(2):1424–1447, 2009.

[18] L.C. Evans. *Partial Differential Equations, Graduate Studies in Mathematics, Vol. 19, American Mathematical Society.* 2009.

[19] L. Faravelli. Response-surface approach for reliability analysis. *Journal of Engineering Mechanics*, 115(12):2763–2781, 1989.

[20] G.S. Fishman. *Monte Carlo: Concepts, Algorithms, and Applications.* Springer, 1996.

[21] P. Frauenfelder, C. Schwab, and R.A. Todor. Finite elements for elliptic problems with stochastic coefficients. *Computer methods in applied mechanics and engineering*, 194(2-5):205–228, 2005.

[22] R.G. Ghanem and P.D. Spanos. *Stochastic Finite Elements: a Spectral Approach.* Dover Civil and Mechanical Engineering, Courier Dover Publications, 2003.

[23] L. Giraud, and J. Langou, and M. Rozložník, and J. van den Eshof. Rounding error analysis of the classical Gram-Schmidt orthogonalization process. *Numerische Mathematik*, 101(1):87–100, 2005.

[24] M.A. Grepl, Y. Maday, N.C. Nguyen, and A.T. Patera. Efficient reduced-basis treatment of nonaffine and nonlinear partial differential equations. *ESAIM: Mathematical Modelling and Numerical Analysis*, 41(03):575–605, 2007.

[25] M.A. Grepl and A.T. Patera. A posteriori error bounds for reduced-basis approximations of parametrized parabolic partial differential equations. *ESAIM: Mathematical Modelling and Numerical Analysis*, 39(01):157–181, 2005.

[26] B. Haasdonk and M. Ohlberger. Reduced basis method for finite volume approximations of parametrized linear evolution equations. *ESAIM: Mathematical Modelling and Numerical Analysis*, 42(02):277–302, 2008.

[27] D.B.P Huynh, G. Rozza, S. Sen, and A.T. Patera. A successive constraint linear optimization method for lower bounds of parametric coercivity and inf-sup stability constants. *Comptes Rendus Mathematique, Analyse Numérique*, 345(8):473–478, 2007.

[28] T. Lassila, A. Quarteroni, and G. Rozza. A reduced basis model with parametric coupling for fluid-structure interaction problems. *SIAM Journal on Scientific Computing*, 34(2):1187–1213, 2012.

[29] J. Li, J. Li, and D. Xiu. An efficient surrogate-based method for computing rare failure probability. *Journal of Computational Physics*, 230(24):8683–8697, 2011.

[30] J. Li and D. Xiu. Evaluation of failure probability via surrogate models. *Journal of Computational Physics*, 229(23):8966–8980, 2010.

[31] Y. Maday, N.C. Nguyen, A.T. Patera, and G.S.H. Pau. A general, multipurpose interpolation procedure: the magic points. *Communications on Pure and Applied Analysis*, 8(1):383–404, 2009.

[32] L. Mathelin and O. Le Maître. Dual-based a posteriori error estimate for stochastic finite element methods. *Communications in Applied Mathematics and Computational Science*, 2(1):83–115, 2007.

[33] H.G. Matthies and A. Keese. Galerkin methods for linear and nonlinear elliptic stochastic partial differential equations. *Computer Methods in Applied Mechanics and Engineering*, 194(12-16):1295–1331, 2005.

[34] F. Nobile, R. Tempone, and C.G. Webster. An anisotropic sparse grid stochastic collocation method for partial differential equations with random input data. *SIAM Journal on Numerical Analysis*, 46(5):2411–2442, 2008.

[35] F. Nobile, R. Tempone, and C.G. Webster. A sparse grid stochastic collocation method for partial differential equations with random input data. *SIAM Journal on Numerical Analysis*, 46(5):2309–2345, 2008.

[36] A. Nouy. A generalized spectral decomposition technique to solve a class of linear stochastic partial differential equations. *Computer Methods in Applied Mechanics and Engineering*, 196(45-48):4521–4537, 2007.

[37] A. Nouy. Recent developments in spectral stochastic methods for the numerical solution of stochastic partial differential equations. *Archives of Computational Methods in Engineering*, 16(3):251–285, 2009.

[38] A. Nouy, A. Clement, F. Schoefs, and N. Moës. An extended stochastic finite element method for solving stochastic partial differential equations on random domains. *Computer Methods in Applied Mechanics and Engineering*, 197(51-52):4663–4682, 2008.

[39] J.T. Oden and S. Prudhomme. Goal-oriented error estimation and adaptivity for the finite element method. *Computers & Mathematics with Applications*, 41(5):735–756, 2001.

[40] J.T. Oden and K.S. Vemaganti. Estimation of local modeling error and goal-oriented adaptive modeling of heterogeneous materials: I. error estimates and adaptive algorithms. *Journal of Computational Physics*, 164(1):22–47, 2000.

[41] A.T. Patera and G. Rozza. Reduced basis approximation and a posteriori error estimation for parametrized partial differential equations Version 1.0. *Copyright MIT, http://augustine.mit.edu*, 2007.

[42] A. Quarteroni. *Numerical Models for Differential Problems.* Springer, MS & A, vol 2, 2009.

[43] A. Quarteroni and G. Rozza. Numerical solution of parametrized Navier–Stokes equations by reduced basis methods. *Numerical Methods for Partial Differential Equations*, 23(4):923–948, 2007.

[44] A. Quarteroni, G. Rozza, and A. Manzoni. Certified reduced basis approximation for parametrized partial differential equations and applications. *Journal of Mathematics in Industry*, 1(1):1–49, 2011.

[45] A. Quarteroni and A. Valli. *Numerical Approximation of Partial Differential Equations.* Springer, 1994.

[46] R. Rackwitz. Reliability analysis review and some perspectives. *Structural Safety*, 23(4):365–395, 2001.

[47] C.P. Robert and G. Casella. *Monte Carlo statistical methods*, volume 2. Springer, 1999.

[48] D.V. Rovas, L. Machiels, and Y. Maday. Reduced-basis output bound methods for parabolic problems. *IMA journal of numerical analysis*, 26(3):423–445, 2006.

[49] G. Rozza. *Shape design by optimal flow control and reduced basis techniques: Applications to bypass configurations in haemodynamics*. PhD thesis, EPFL, 2005.

[50] G. Rozza, D.B.P. Huynh, and A.T. Patera. Reduced basis approximation and a posteriori error estimation for affinely parametrized elliptic coercive partial differential equations. *Archives of Computational Methods in Engineering*, 15(3):229–275, 2008.

[51] Y. Saad. *Iterative methods for sparse linear systems*, volume 620. PWS publishing company Boston, 1996.

[52] G.I. Schuëller, H.J. Pradlwarter, and P.S. Koutsourelakis. A critical appraisal of reliability estimation procedures for high dimensions. *Probabilistic Engineering Mechanics*, 19(4):463–474, 2004.

[53] C. Schwab and R. A. Todor. Karhunen-Loève approximation of random fields by generalized fast multipole methods. *Journal of Computational Physics*, 217(1):100–122, 2006.

[54] C. Schwab and R.A. Todor. Sparse finite elements for elliptic problems with stochastic loading. *Numerische Mathematik*, 95(4):707–734, 2003.

[55] G. Stefanou. The stochastic finite element method: past, present and future. *Computer Methods in Applied Mechanics and Engineering*, 198(9-12):1031–1051, 2009.

[56] Terence Tao and Van Vu. Random matrices: Universality of local eigenvalue statistics. *Acta mathematica*, 206(1):127–204, 2011.

[57] D. Xiu and G. Em Karniadakis. Modeling uncertainty in steady state diffusion problems via generalized polynomial chaos. *Computer Methods in Applied Mechanics and Engineering*, 191(43):4927–4948, 2002.

[58] D. Xiu and J.S. Hesthaven. High-order collocation methods for differential equations with random inputs. *SIAM Journal on Scientific Computing*, 27(3):1118–1139, 2005.

[59] D. Xiu and G.E. Karniadakis. The Wiener-Askey polynomial chaos for stochastic differential equations. *SIAM Journal on Scientific Computing*, 24(2):619–644, 2003.

[60] S. Zhang. Efficient greedy algorithms for successive constraints methods with high-dimensional parameters. *Brown Division of Applied Math Scientific Computing Tech Report*, 23, 2011.

MATHEMATICS INSTITUTE OF COMPUTATIONAL SCIENCE AND ENGINEERING
Section of Mathematics
Ecole Polytechnique Fédérale
CH-1015 Lausanne

47.2012 A. ABDULLE, Y. BAI:
Fully discrete analysis of the heterogeneous multiscale method for elliptic problems with multiple scales

48.2012 G. MIGLORATI, F. NOBILE, E. VON SCHWERIN, R. TEMPONE:
Approximation of quantities of interest in stochastic PDES by the random discrete L^2 projection on polynomial spaces

01.2013 A. ABDULLE, A. BLUMENTHAL:
Stabilized multilevel Monte Carlo method for stiff stochastic differential equations

02.2013 D. N. ARNOLD, D. BOFFI, F. BONIZZONI:
Tensor product finite element differential forms and their approximation properties

03.2013 N. GUGLIELMI, D. KRESSNER, C. LUBICH:
Low-rank differential equations for Hamiltonian matrix nearness problems

04.2013 P. CHEN, A. QUARTERONI, G. ROZZA:
A weighted reduced basis method for elliptic partial differential equations with random input data

05.2013 P. CHEN, A. QUARTERONI, G. ROZZA:
A weighted empirical interpolation method: a priori convergence analysis and applications

06.2013 R. SCHNEIDER, A. USCHMAJEW:
Approximation rates for the hierarchical tensor format in periodic Sobolev spaces

07.2013 C. BAYER, H. HOEL, E. VON SCHWERIN, R. TEMPONE:
On non-asymptotic optimal stopping criteria in Monte Carlo simulation.

08.2013 L. GRASEDYCK, D. KRESSNER, C. TOBLER:
A literature survey of low-rank tensor approximation techniques

09.2013 M. KAROW, D. KRESSNER:
On a perturbation bound for invariant subspaces of matrices

10.2013 A. ABDULLE:
Numerical homogenization methods

11.2013 PH. BLANC:
Lower bound for the maximum of some derivative of Hardy's function

12.2013 A. ABDULLE, Y. BAI, G. VILMART:
Reduced basis finite element heterogeneous multiscale method for quasilinear elliptic homogenization problems

13.2013 P. CHEN, A. QUARTERONI:
Accurate and efficient evaluation of failure probability for partial different equations with random input data